Available online at www.sciencedirect.com
ScienceDirect
Biochemical and Biophysical Research Communications 353 (2007) 182–188
BBRC
www.elsevier.com/locate/ybbrc

A novel approach for myocardial regeneration with educated cord blood cells cocultured with cells from brown adipose tissue

Yoshihiro Yamada [a,*], Shin-ichiro Yokoyama [b], Noboru Fukuda [b], Hiroyasu Kidoya [a], Xiao-Yong Huang [a], Hisamichi Naitoh [a], Naoyuki Satoh [a], Nobuyuki Takakura [a,*]

[a] *Department of Signal Transduction, Research Institute for Microbial Diseases, Osaka University, 3-1 Yamadaoka, Suita-shi, 565-0871, Japan*
[b] *Second Department of Internal Medicine, Nihon University School of Medicine, Ooyaguchi-kami 30-1, Itabashi-ku, Tokyo 173-8610, Japan*

Received 22 November 2006
Available online 11 December 2006

Abstract

Umbilical cord blood (CB) is a promising source for regeneration therapy in humans. Recently, it was shown that CB was a source of mesenchymal stem cells as well as hematopoietic stem cells, and further that the mesenchymal stem cells could differentiate into a number of cells types of mesenchymal lineage, such as cardiomyocytes (CMs), osteocytes, chondrocytes, and fat cells. Previously, we reported that brown adipose tissue derived cells (BATDCs) differentiated into CMs and these CMs could adapt functionally to repair regions of myocardial infarction. In this study, we examined whether CB mononuclear cells (CBMNCs) could effectively differentiate into CMs by coculturing them with BATDCs and determined which population among CBMNCs differentiated into CMs. The results show that BATDCs effectively induced CBMNCs that were non-hematopoietic stem cells (HSCs) (educated CB cells: e-CBCs) into CMs in vitro. E-CBCs reconstituted infarcted myocardium more effectively than non-educated CBMNCs or CD34-positive HSCs. Moreover, we found that e-CBCs after 3 days coculturing with BATDCs induced the most effective regeneration for impaired CMs. This suggests that e-CBCs have a high potential to differentiate into CMs and that adequate timing of transplantation supports a high efficiency for CM regeneration. This strategy might be a promising therapy for human cardiac disease.

Keywords: Stem cell; Cord blood; Adipose tissue; Myocardial regeneration; Cell fusion

Myocardial regeneration is currently a popular topic in cardiac medicine, and research in regenerative medicine has advanced in an explosive manner. Many cell types such as bone marrow mesenchymal stem cells (BM-MSCs) [1–3], embryonic stem (ES) cells [4,5], and cardiac tissue stem cells [6,7] have been found to undergo myocardial differentiation and can be used as a source for cardiomyocytes (CMs). Additional cell types may also prove to have cardiac differentiation ability. With regard to human therapy, umbilical cord blood (CB) is a promising source because transplantation of CB has already been established for patients with blood diseases. Moreover, usage of CB overcomes considerable problems encountered with other sources of CMs, such as allergenic, ethical, and tumorigenic issues. Furthermore, CB contains both hematopoietic stem cells (HSCs) [8] and MSCs [9]. Also, stem cells are more abundant in CB than in adult human peripheral blood or bone marrow (BM) and stem cells in CB have a higher proliferative potential associated with an extended life span and longer telomeres [10–12].

Indeed, $CD34^+$ cells derived from human CB homed to infarcted hearts and reduced the size of the infarcted area; this was not through direct differentiation into CMs, but through enhancing neovascularization [13,14]. These studies showed no evidence of myocytes of human origin in the infracted myocardium; however, it was reported that unrestricted somatic stem cells (USSCs) from human CB could differentiate into CMs in vitro and in vivo [15]. Such

* Corresponding authors. Fax: +81 6 6879 8314.
E-mail addresses: yamaday@biken.osaka-u.ac.jp (Y. Yamada), ntakaku@biken.osaka-u.ac.jp (N. Takakura).

0006-291X/$ - see front matter © 2006 Elsevier Inc. All rights reserved.
doi:10.1016/j.bbrc.2006.12.017

USSCs are fibroblastic in appearance and negative for hematopoietic cell markers, such as c-kit, CD34, and CD45. USSCs injected into immunosuppressed pig model of myocardial infarction (MI) improved perfusion and wall motion, reduced infarct scar size, and enhanced cardiac function. USSCs seem to be a useful source for myocardial regeneration; however, they are a rare population, therefore, expansion of USSCs is required for application to clinical therapy. In spite of these challenges for the repair of CM, to date, no clinical studies of CB have been reported. Previously, we reported that brown adipose tissue derived cells (BATDCs) included cardiac progenitor cells and they effectively differentiated into CMs in vitro and in vivo [16]. This indicated that our culture system of BATDCs contained differentiation molecular cues for CMs. When BATDCs were injected into MI rats, they differentiated into CMs as well as endothelial cells (ECs) and smooth muscle cells (SMCs), supported the growth of resident cells and vascular cells, and restored cardiac function. This suggested a potential therapeutic use for BATDCs in human ischemic heart disease. However, in humans, BAT exists only in the embryonic stage and infants, therefore, it is difficult to obtain BATDCs to treat adult cardiac disease. In this study, we examined whether mononuclear cells from CB can differentiate into CMs upon coculturing with BATDCs. Moreover, usefulness of CB cells that were exposed to BATDCs for MI repair was evaluated.

Materials and methods

Cell preparation and flow cytometry. Brown adipose tissue (BAT) was dissected from postnatal day (P1) to P7 neonates of C57BL/6 mice. BAT was dissociated by DispaseII (Roche, Mannheim, Germany), drawn through a 23G needle and prepared as single cell suspension as previously reported [16]. Human CB mononuclear cells (CBMNCs) were purchased from Cambrex (Baltimore, MD). The cell-staining procedure for the flow cytometry was also as previously described [17]. The monoclonal antibodies (mAbs) used in immunofluorescence staining were anti-human CD45, -34, and -HLA–ABC mAbs (Pharmingen, SanDiego, CA). All mAbs were purified and conjugated with fluorescein isothiocyanate (FITC), PE (phycoerythrin), biotin or allophycocyanin (APC). Biotinylated antibodies were visualized with PE-conjugated streptavidin (Pharmingen) or APC-conjugated streptavidin (Pharmingen). Cells were incubated for 5 min on ice with CD16/32 (FcγIII/II Receptor) (1:100) (Fcblock™, Pharmingen) prior to staining with primary antibody. Cells were incubated in 5% fetal calf serum/phosphate-buffered saline (FCS/PBS; washing buffer) with primary antibody for 30 min on ice, and washed twice with washing buffer. Secondary antibody was added and the cells were incubated for 30 min on ice. After incubation, cells were washed twice with, and suspended in, the washing buffer for fluorescence-activated cell sorter (FACS) analysis. The stained cells were analyzed and sorted by EPICS Flowcytometer (BECKMAN COULTER, San Jose, CA). The sorted cells were added to 24-well dishes (Nunc, Roskilde, Denmark), precoated with 0.1% gelatin (Sigma, St. Louis, USA), and cultured in Dulbecco's modified Eagle's medium (DMEM; Sigma), supplemented with 10% FCS and 10^{-5}M 2-mercaptoethanol (2-ME), at 37 °C in a 5% CO_2 incubator.

Cell coculture. BATDCs were prepared as described above. When BATDCs and human (h) CBMNCs were cocultured in contact conditions, 1×10^5 BATDCs were plated per well of a 24-well plate and cultured for 7 days, and then, 1×10^5 CBMNCs, or 1×10^4 $CD34^+$ HSCs were cultured with BATDCs for 10 days. Staining was performed with anti-cardiac troponinT (Santa Cruz), -MEF-2C (Cell signaling) and -HLA ABC antibodies (Pharmingen).

Supplemental information reveals the Materials and methods for RT-PCR analysis, Immunohistochemistry, FISH staining, and procedure for mouse myocardial infarction (MI) model and echocardiography.

Results

Differentiaion of CBMNCs into CMs by coculturing with BATDCs in vitro

Previously, we reported that BATDCs differentiate into CMs spontaneously; this suggests that BATDCs produce molecules that induce self differentiation into CMs by an autocrine loop. Moreover, CBMNCs contained cells with a potential to differentiate into various cell types, such as osteoblasts, chondrocytes, and CMs. Therefore, to determine whether molecules produced from BATDCs induce CBMNCs to differentiate into CMs effectively, we cultured CBMNCs with BATDCs and observed the differentiation of CBMNCs into CMs. At first, dissociated BATDCs from P1 to P7 neonatal mice were cultured on 0.1% gelatin-coated dishes. After 1 week, human CBMNCs were added and cocultured with BATDCs. After coculturing CBMNCs with BATDCs for 14 days, among HLA-positive CBMNCs, nuclear located MEF2C positive and cardiac troponinT-positive cells (Fig. 1A and B), or cardiac troponinI-positive cells (Fig. 1C) were effectively produced. In contrast, sorted $CD34^+38^-$HSC population from CBMNCs, which was previously reported to differentiate into CMs [18], was differentiated into cardiac troponinT-positive CMs (Fig. 1E); however, the frequency of CM differentiation from HSC population was lower than that from total CBMNCs (Fig. 1I). CBMNCs alone did not differentiate into cardiac troponinT-positive or MEF2C-positive cells spontaneously under the same culture medium without coculturing with BATDCs (Fig. 1G, H, and I).

The expression of CM-specific genes in CBMNCs educated by culturing with BATDCs

Next, we evaluated the length of time required for CBMNCs to become committed CM lineage cells when cocultured with BATDCs. For this purpose, we attempted to coculture CBMNCs with BATDCs for 1 to 7 days and $HLA^+CD45^-CD34^-$ non-hematopoietic cells [we termed them educated CB cells (e-CBCs)] were then sorted and mRNA was extracted from the cells as indicated in Fig. 2A. Because mature hematopoietic cells from cocultured CBMNCs did not differentiate into CMs (data not shown) and HSC population barely differentiated into CMs (Fig. 1), we deduced that cardiac stem/progenitor cells were more abundant in non-hematopoietic cells and were therefore $CD45^-CD34^-$. We analyzed the expression of CM-specific genes on days 0, 3, and 7 as indicated in Fig. 2B and confirmed that cardiac actin, myosin light chain 2v, and specific transcriptional factor, such as

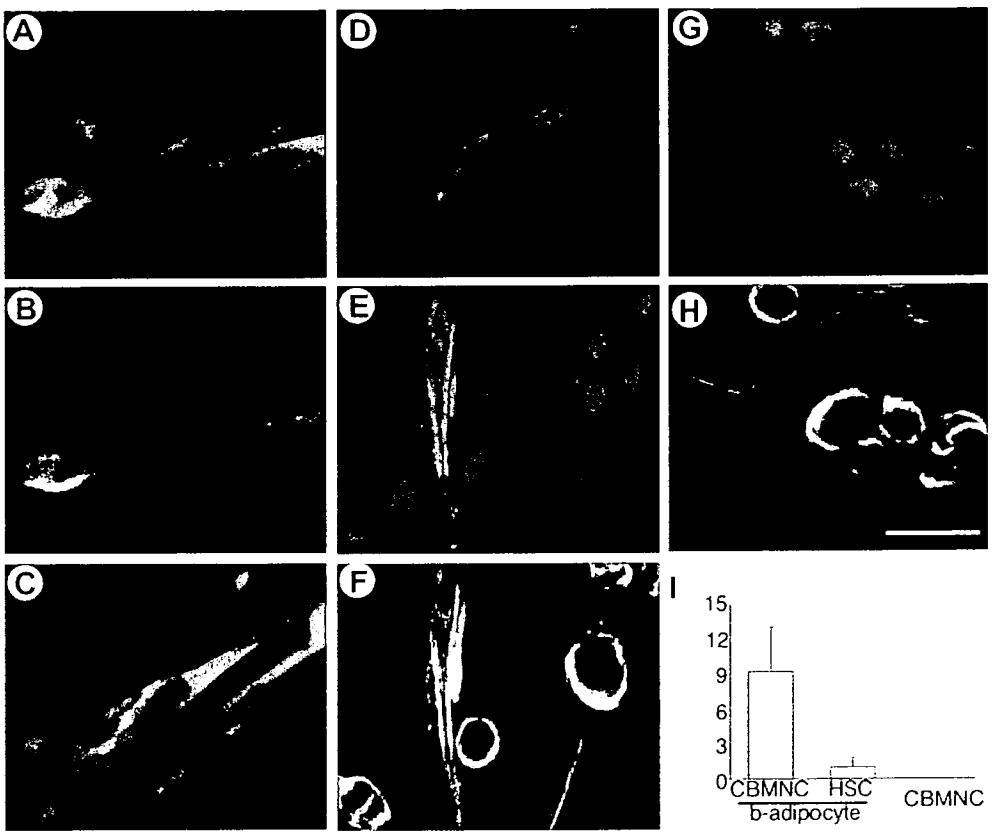

Fig. 1. CBMNCs can differentiate into CMs upon coculturing with BATDCs. Immunocytochemical analysis of human CBMNCs (A–D), and $CD34^+CD38^-$HSCs (E, F) cocultured with BATDCs from wild type mice, or CBMNCs (G, H) cultured without BATDCs for 14 days. (A) Expression of cardiac troponinT (green) and MEF2C (red). (B) Human HLA expression (blue) in the same field as (A). (C, E, and G) Expression of cardiac troponinI (green) and nuclear staining with PI (red). (D, F, and H) Human HLA expression (blue) in the same fields as (C, E, and G), respectively. Scale bar in (H) indicates 5 μm. (I) Quantitative evaluation of differentiated cardiac troponinT and MEF2C-positive CMs among adhering HLA-positive CB-derived cells. Data for CBMNC, and $CD34^+CD38^-$HSCs cocultured with BATDCs (b-adipocyte) and CBMNCs cultured without BATDCs are displayed. Results represent means ± SD of five independent experiments.

GATA-4 and Nkx2.5 were expressed on day 3 of coculture (Fig. 2B). MHC alpha and beta mRNAs were not expressed on day 3; however, they started to be expressed around day 7.

Educated CBMNCs in non-hematopoietic lineage contributed to myocardial regeneration

As indicated in Fig. 2, 3 days of coculturing with BATDCs was enough for commitment of CBMNCs into CM lineage. Next, in order to determine whether e-CBCs could effectively contribute to the regeneration of the heart, we injected the e-CBCs into the hearts of nude rats after the induction of an acute MI as indicated in Fig. 3A. At first, we cocultured CBMNCs with BATDCs for 3 days, purified $HLA^+CD45^-CD34^-$ cells (e-CBCs) by FACS and injected the cells into the hearts of experimental MI nude rats at each of five sites at the border of the infarcted tissue. As a control, infarcted hearts were injected with either equal volumes and numbers of CBMNCs that were not exposed to BATDCs (non-e-CBCs), or $CD34^+38^-$HSCs directly sorted from freshly isolated CBMNCs. Upon injection of e-CBCs, donor-derived human HLA- and SA-positive cells were detected abundantly in the infarct border zone (Fig. 3B, a, b, and c; 23.4 ± 3.1% of total cardiomyocytes in one field), but the contribution to CMs by the injection with non-e-CBCs and $CD34^+38^-$HSCs in the MI was 20- (Fig. 3B, d, e, and f; 1.1 ± 0.3%) and 15-fold (Fig. 3B, g, h, and i; 1.5 ± 0.3%), respectively, less than that of e-CBCs. e-CBC-derived SA-positive CMs also expressed connexin 43 (Fig. 3Bc), indicating that transplanted e-CBC-derived CMs formed gap junctions with host CMs. Moreover, the assessment of cardiac function by echocardiography revealed that the hearts injected with e-CBCs showed improved contractions of movement of the infarcted anterior walls and reduced left ventricular remodeling compared with the hearts injected with non-e-CBCs or $CD34^+38^-$HSCs (Fig. 4).

To clarify the origin of CMs in recipient tissue, donor-derived human chromosomes and host-derived rat chromosomes were simultaneously detected by using species-specific chromosome probes using fluorescent in situ hybridization (FISH) analysis. In this analysis, we used centromere probes, because 5 μm thick slices may not always include sex chromosomes in the nuclei as previously described [18]. Result showed that

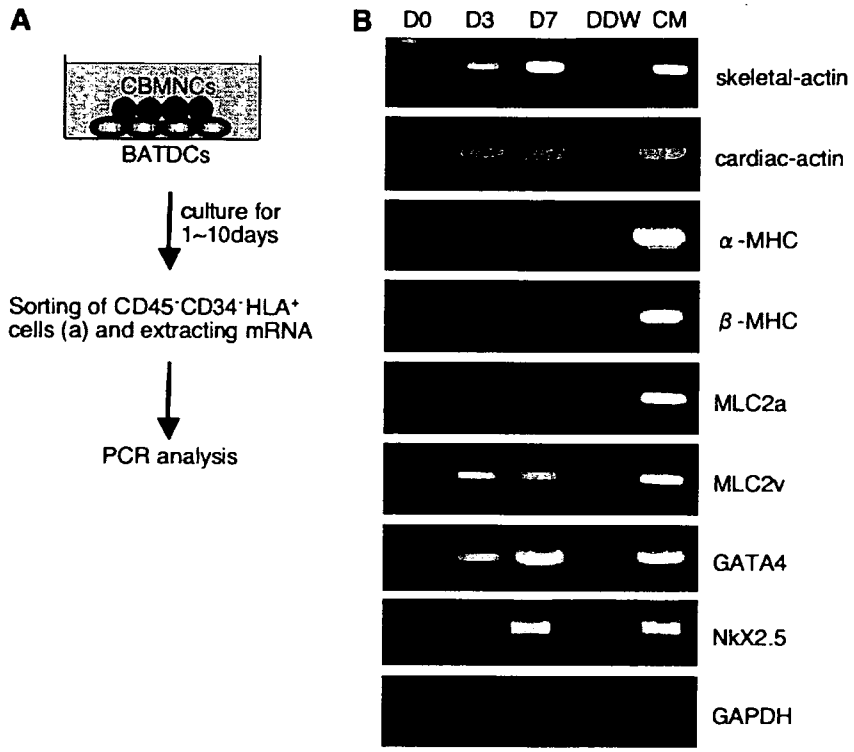

Fig. 2. Expression of CM-specific genes in e-CBCs. (A) Design of experiment for the isolation of human e-CBCs. CBMNCs were cocultured with BATDCs for 1 to 10 days, and then $CD45^{-}CD34^{-}$ human HLA^{+} cells were sorted and total RNA was extracted. (B) PCR analysis was performed with CM-specific primers in e-CBCs after coculturing with BATDCs for 0 day (D0; freshly isolated CBCs without exposure to BATDCs), 3 days (D3) and 7 days (D7). Distilled water (DDW) and CMs from embryos (CM) were used as a negative and a positive control, respectively. GAPDH was used as an internal control.

implanted e-CBCs of human origin transferred into female nude rats formed CMs that stained only with probes specific for human chromosomes (Fig. 3C, a and b). We also checked the serial confocal imaging to exclude the possibility that they arose from cell overlay as previously reported [18], but could not observe any superimposed cells (data not shown). This indicated that in vivo cardiac differentiation of e-CBCs was not induced by the fusion mechanism. In contrast, when $CD34^{+}CD38^{-}$HSCs were implanted into MI induced nude rats, human HLA-positive CMs were stained with both human and rat chromosome probes (data not shown). This indicated that generation of CM-derived HSCs was due to the fusion mechanism between donor-derived cells and host CMs as previously reported [18,19].

Discussion

So far, various kinds of sources for CMs, such as adult BM HSCs [19,20], MSCs [1–3], and ES cells [4,5] have been reported; however, there is some controversy regarding the efficiency of cardiomyoplasty. In terms of the myocardial regeneration therapy for human, human CB cells seem to be a safe and useful source compared to other sources, because these cells have already been utilized in CB transplantation for managing patients with blood disease. However, no clinical trials using CB cells to treat heart disease have been reported.

In this study, we raised two important points. The first is that e-CBCs of non-hematopoietic origin were more effectively differentiated into CMs compared with $CD34^{+}CD38^{-}$HSCs in vitro. Moreover, we showed that e-CBCs differentiation into CMs was not through the cell fusion mechanism. On the other hand, CMs derived from $CD34^{+}CD38^{-}$HSCs were generated through cell fusion with host CMs in vivo. Previously, it was reported that MSCs but not HSCs from BM could migrate into the heart and differentiate into CMs in mouse MI model [21]. This suggested that MSCs were the predominant source for myocardial regeneration. Our report is the first to show that non-hematopoietic cells can be used as CM source and how these compare with HSCs in human cord blood cells.

The second is the new strategy for myocardial regeneration using CB cells and BATDCs. Using the coculturing method described here, CB cells were effectively induced to differentiate into CMs in vitro. Moreover, e-CBCs were effectively differentiated into CMs in immunodeficient rat MI model and improved the cardiac function. Furthermore, we found that an adequate duration of coculturing of CB cells with BATDCs was critical for CM regeneration. In the present method, three days of coculturing was the most effective to produce CMs from e-CBCs and improve the CM function and this timing was consistent

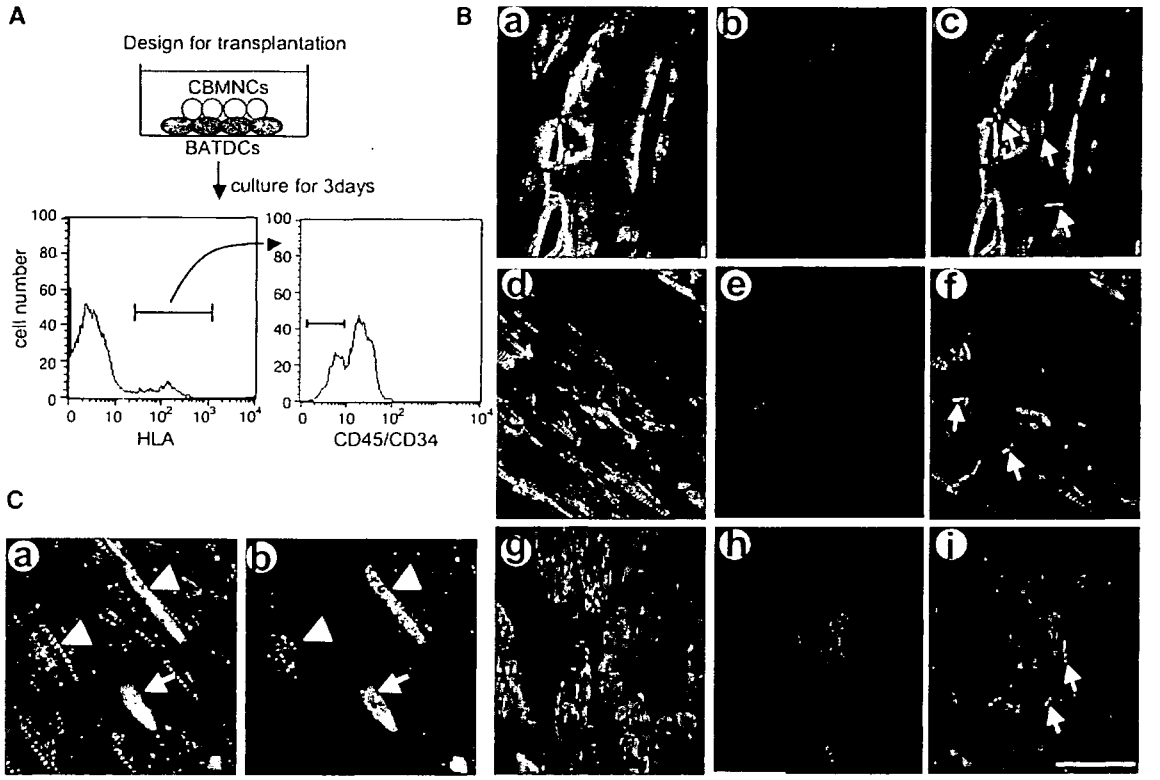

Fig. 3. CBMNCs cocultured with BATDCs contributed to cardiac regeneration. (A) Strategy for transplantation. After human CBMNCs were cocultured for 3 days with BATDCs from mice, human $HLA^+CD45^-CD34^-$ cells (e-CBCs) were sorted by FACS and injected into the border zone of ischemia induced nude rats. As a control, CBMNCs that were not coclured (non-e-CBCs) and freshly isolated $CD34^+CD38^-$HSCs were used. (B) CM development from injected e-CBCs (a–c), non-e-CBCs (d–f), and $CD34^+CD38^-$HSCs in MI induced heart. (a, d, and g) Expression of SA (green), (b, e, and h) human HLA (red). (c, f, and i) are merged image of (a and b), (d and e), and (g and h), respectively, and stained with anti-connexin 43 antibody (blue). Arrows in (c, f, and i) indicate the regions in which human CB-derived connexin positive CMs make tight junction with resident host CMs. Scale bar in (i) indicates 20 μm. (C) (a) Expression of human HLA (red) and SA (green) in the site of implantation of e-CBCs in MI induced heart. Nuclei were counter stained with TOPRO3 (blue). (b) FISH staining in a serial section of (a). Green colors indicate rat chromosome, and red color indicates human chromosome. Nuclear staining was performed with TOPRO3 (blue). Cells expressing human chromosome (red) in the nuclei indicate that these cells were derived from e-CBCs and did not fuse with host CM expressing only rat chromosome (green). Arrowheads indicate nuclei from host CMs and arrow indicates human nuclei in e-CBCs (a, b). Scale bar indicates 5 μm.

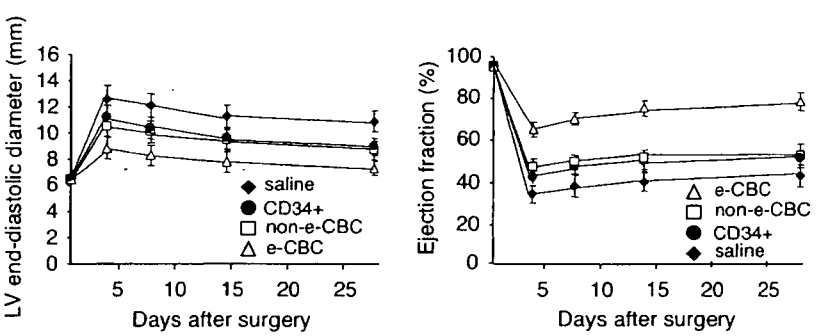

Fig. 4. e-CBCs transplantation improved cardiac function. LV diameter (LV end-diastolic diameter) and function (Ejection fraction) were assessed by echocardiography at 0, 3, 7, 14, and 28 days following myocardial infarction and injection of saline, e-CBCs, non-e-CBCs, and HSCs (CD34+). Note that in case of injection of e-CBCs, enlargement of LV diameter was reduced and LV function was significantly improved compared with injection of saline, non-e-CBCs, and HSCs. Each data point is the mean of five determinations; bars denote ±SD.

with the expression of Nkx2.5 and GATA-4 on CBMNCs (Fig. 2). In order to determine how e-CBCs differentiated into CMs, we tested a number of growth and survival factors and found that Akt activation seemed to play a role in the differentiation of CBMNCs into CMs (Supplemental data 1). Akt, a serine threonine kinase, transduces powerful survival signals in many systems [22,23]. Recently, it was reported that overexpression of Akt1 in MSCs increased the post-transplantation viability of these cells and enhanced their therapeutic efficiency [24]. In fact, intramyocardial injection of MSCs that had been transfected with a retroviral vector containing the Akt gene resulted in the

differentiation of MSCs into CMs and led to the prevention of ventricular remodeling and to the restoration of cardiac function after MI. In order to examine the survival signals in e-CBCs in each culture day as indicated, we checked the phosphorylation level of Akt (p-Akt) in e-CBCs on days 0, 3, and 7. Before extraction of cell lysate, e-CBCs were exposed to hypoxic condition for 24 h. The p-Akt level of e-CBCs on day 3 was 10-fold higher than that on day 7 and it was higher (1.7×) than that on day 0 before coculturing with BATDCs (Supplement data 1). The resistance of cell to apoptosis induced by hypoxic stimuli was proportional to the level of p-Akt in e-CBCs, i.e., it was higher on day 3 compared to day 0 and day 7. This anti-apoptotic effect might contribute to the high incidence of CMs derived from e-CBCs and to prevention of cardiac remodeling caused by conditions such as hypoxia, inflammation, and mechanical stress, and many endogenous factors such as angiotensin II, endothelin-1, and norepinephrine [25] in MI model.

We have as yet not clarified the precise mechanism whereby CB cells expressed high levels of p-Akt in hypoxic conditions after short-term coculturing with BATDCs. BATDCs were derived from adipose tissue, which possessed many beneficial factors, such as vascular endothelial growth factor (VEGF), hepatocyte growth factor (HGF), angiopoietin-1, and so on [16]. Therefore, these factors might support the high level of p-Akt in e-CBCs. Identification of such factors may enable effective myocardial regeneration. Use of CBCs together with such factors for protection against cell apoptosis may enable the application of the strategy described here to the clinic for managing patients of ischemic disease.

Acknowledgments

We thank Miss M. Sato for technical support. This study was supported in part by a grant from the Ministry of Education, Culture, Sports, Science, and Technology of Japan.

Appendix A. Supplementary data

Supplementary data associated with this article can be found, in the online version, at doi:10.1016/j.bbrc.2006.12.017.

References

[1] S. Makino, K. Fukuda, S. Miyoshi, F. Konishi, H. Kodama, J. Pan, M. Sano, T. Takahashi, S. Hori, H. Abe, J. Hata, A. Umezawa, S. Ogawa, Cardiomyocytes can be generated from marrow stromal cells in vitro, J. Clin. Invest. 103 (1999) 697–705.

[2] C. Toma, M.F. Pittenger, K.S. Cahill, B.J. Byrne, P.D. Kesseler, Human mesencymal stem cells differentiate to a cardiomyocyte phenotype in adult murine heart, Circulation 105 (2002) 93–98.

[3] S. Tomita, R.K. Li, R.D. Weise, D.A. Mickle, E.J. Kim, T. Sakai, Z.Q. Jia, Autologous transplantation of bone marrow cells improves damaged heart function, Circulation 100 (1999) 247–256.

[4] I. Kehat, D. Kenyagin-Karsenti, M. Snir, M. Segev, M. Amit, A. Gepstein, E. Livne, O. Binah, J. Itskovitz-Eldor, L. Gepstein, Human embryonic stem cells can differentiate into myocytes with structural and functional properties of cardiomyocytes, J. Clin. Invest. 108 (2001) 407–414.

[5] I. Kehat, A. Gepstein, A. Spira, J. Itskovitz-Eldor, L. Gepstein, High-resolution electrophysiological assessment of human embryonic stem cell-derived cardiomyocytes: a novel in vitro model for the study of conduction, Circ. Res. 91 (2002) 659–661.

[6] A.P. Beltrami, L. Barlucchi, D. Torella, M. Baker, F. Limana, S. Chimenti, H. Kasahara, M. Rota, E. Musso, K. Urbanek, A. Leri, J. Kajstura, B. Nadal-Ginard, P. Anversa, Adult cardiac stem cells are multipotent and support myocardial regeneration, Cell 114 (2003) 763–776.

[7] H. Oh, S.B. Bradfute, T.D. Gallardo, T. Nakamura, V. Gaussin, Y. Mishina, J. Pocius, L.H. Michael, R.R. Behringer, D.J. Garry, M.L. Entman, M.D. Schneider, Cardiac progenitor cells from adult myocardium: homing, differentiation, and fusion after infarction, Proc. Natl. Acad. Sci. USA 100 (2003) 12313–12318.

[8] H. Mayani, P.M. Lansdorp, Biology of human umbilical cord blood derived hematopoietic stem/progenitor cells, Stem Cells 16 (1998) 153–165.

[9] A. Erices, P. Congnet, J.J. Minguell, Mesenchymal progenitor cells in human umbilical cord blood, Br. J. Haemotol. 109 (2000) 235–242.

[10] S.J. Szilvassy, T.E. Meyerrose, P.L. Ragland, B. Grimes, Differentioal homing and engraftment properties of hematopoietic progenitor cells from murine bone marrow, mobilized peripheral blood, and fetal liver, Blood 98 (2001) 2108–2115.

[11] H. Vaziri, W. Dragowska, R.C. Allsopp, T.E. Thomas, C.B. Harley, P.M. Lansdorp, Evidence for a mitotic clock in human hematopoietic stem cells: loss of telomeric DNA with age, Proc. Natl. Acad. Sci. USA 91 (1994) 9857–9860.

[12] E.D. Zanjani, J.L. Ascensao, M. Tavassoli, Liver derived feta hematopoietic stem cells selectively and preferentially home to the fetal bone marrow, Blood 81 (1993) 399–404.

[13] N. Ma, Y. Ladilov, J.M. Moebius, L. Ong, C. Piechaczek, A. David, A. Kaminski, Y.H. Choi, W. Li, D. Egger, C. Stamm, G. Steinhoff, Intramyocardial delivery of human CD133+ cells in a SCID mouse cryoinjury model: bone marrow vs. cord blood-derived cells, Cardiovasc. Res. 71 (2006) 158–169.

[14] Y. Hirata, M. Sata, N. Motomura, M. Takanashi, Y. Suematsu, M. Ono, S. Takamoto, Human umbilical cord blood cells improve cardiac function after myocardial infarction, Biochem. Biophys. Res. Commun. 327 (2005) 609–614.

[15] G. Kogler, S. Sensken, J.A. Airey, T. Trapp, M. Muschen, N. Feldhahn, S. Liedtke, R.V. Sorg, J. Fischer, C. Rosenbaum, S. Greschat, A. Knipper, J. Bender, O. Degistirici, J. Gao, A.I. Caplan, E.J. Colletti, G. Almeida-Porada, H.W. Muller, E. Zanjani, P. Wernet, A new human somatic stem cell from placental cord blood with intrinsic pluripotent differentiation potential, J. Exp. Med. 200 (2004) 123–135.

[16] Y. Yamada, X.D. Wang, S.-I. Yokoyama, N. Fukuda, N. Takakura, Cardiac Progenitor cells in brown adipose tissue repaired damaged myocardium, Biochem. Biophys. Res.Commun. 343 (2006) 662–670.

[17] Y. Yamada, N. Takakura, H. Yasue, H. Ogawa, H. Fujisawa, T. Suda, Exogenous clustered neuropilin 1 enhances vasculogenesis and angiogenesis, Blood 97 (2001) 1671–1678.

[18] F. Ishikawa, H. Shimazu, L.D. Shultz, M. Fukata, R. Nakamura, B. Lyons, K. Shimoda, S. Shimoda, T. Kanemaru, K. Nakamura, H. Ito, Y. Kaji, A.C. Perry, M. Harada, Purified human hematopoietic stem cells contribute to the generation of cardiomyocytes through cell fusion, FASEB J. 20 (2006) 950–952.

[19] M. Alvarez-Dolado, R. Pardal, J.M. Garcia-Verdugo, J.R. Fike, H.O. Lee, K. Pfeffer, C. Lois, S.J. Morrison, A. Alvarez-Buylla, Fusion of bone-marrow-derived cells with Purkinje neurons, cardiomyocytes and hepatocytes, Nature 425 (2003) 968–973.

[20] D. Orlic, J. Kajstura, S. Chimenti, I. Jakoniuk, S.M. Anderson, B. Li, J. Pickel, R. Mckay, B. Nadal-Ginard, D.M. Bodine, A. Leri, P.

Anversa, Bone marrow cells regenerate infarcted myocardium, Nature 410 (2001) 701–705.
[21] H. Kawada, J. Fujita, K. Kinjo, Y. Matsuzaki, M. Tsuma, H. Miyatake, Y. Muguruma, K. Tsuboi, Y. Itabashi, Y. Ikeda, S. Ogawa, H. Okano, T. Hotta, K. Ando, K. Fukuda, Nonhematopoietic mesenchymal stem cells can be mobilized and differentiate into cardiomyocytes after myocardial infarction, Blood 104 (2004) 3581–3587.
[22] T.F. Franke, D.R. Kaplan, L.C. Cantley, PI3K: downstream AKTion blocks apoptosis, Cell 88 (1997) 435–437.
[23] S.R. Datta, A. Brunet, M.E. Greenberg, Cellular survival: a play in three Akts, Genes Dev. 13 (1999) 2905–2927.
[24] A.A. Mangi, N. Noiseux, D. Kong, H. He, M. Rezvani, J.S. Ingwall, V.J. Dzau, Mesenchymal stem cells modified with Akt prevent remodeling and restore performance of infarcted hearts, Nat. Med. 9 (2003) 1195–1201.
[25] H. Takano, Y. Qin, H. Hasegawa, K. Ueda, Y. Niitsuma, M. Ohtsuka, I. Komuro, Effects of G-CSF on left ventricular remodeling and heart failure after acute myocardial infarction, J. Mol. Med. 84 (2006) 185–193.

Molecular Biology of the Cell
Vol. 18, 1421–1429, April 2007

Prox1 Induces Lymphatic Endothelial Differentiation via Integrin α9 and Other Signaling Cascades[D] [V]

Koichi Mishima,*† Tetsuro Watabe,* Akira Saito,* Yasuhiro Yoshimatsu,* Natsuko Imaizumi,* Shinji Masui,‡ Masanori Hirashima,§ Tohru Morisada,§ Yuichi Oike,§ Makoto Araie,† Hitoshi Niwa,‡ Hajime Kubo,‖ Toshio Suda,§ and Kohei Miyazono*¶

Departments of *Molecular Pathology and †Ophthalmology, Graduate School of Medicine, University of Tokyo, Tokyo 113-0033, Japan; ‡Laboratory for Pluripotent Cell Studies, RIKEN Center for Developmental Biology, Kobe 650-0047, Japan; §Department of Cell Differentiation, The Sakaguchi Laboratory, School of Medicine, Keio University, Shinanomachi, Tokyo 160-8582, Japan; ‖Molecular and Cancer Research Unit, Horizontal Medical Research Organization (HMRO), Graduate School of Medicine, Kawaramachi, Kyoto University, Kyoto 606-8501, Japan; and ¶Department of Biochemistry, The Cancer Institute of the Japanese Foundation for Cancer Research, Ariake, Tokyo 135-8550, Japan

Submitted September 5, 2006; Revised January 2, 2007; Accepted January 31, 2007
Monitoring Editor: Ben Margolis

During embryonic lymphatic development, a homeobox transcription factor Prox1 plays important roles in sprouting and migration of a subpopulation of blood vessel endothelial cells (BECs) toward VEGF-C–expressing cells. However, effects of Prox1 on endothelial cellular behavior remain to be elucidated. Here, we show that Prox1, via induction of integrin α9 expression, inhibits sheet formation and stimulates motility of endothelial cells. Prox1-expressing BECs preferentially migrated toward VEGF-C via up-regulation of the expression of integrin α9 and VEGF receptor 3 (VEGFR3). In mouse embryos, expression of VEGFR3 and integrin α9 is increased in Prox1-expressing lymphatic endothelial cells (LECs) compared with BECs. Knockdown of Prox1 expression in human LECs led to decrease in the expression of integrin α9 and VEGFR3, resulting in the decreased chemotaxes toward VEGF-C. These findings suggest that Prox1 plays important roles in conferring and maintaining the characteristics of LECs by modulating multiple signaling cascades and that integrin α9 may function as a key regulator of lymphangiogenesis acting downstream of Prox1.

INTRODUCTION

The major roles of the lymphatic vessels are to drain interstitial fluid that leaks out from the blood capillaries and to return it to the blood vessels. In addition, the lymphatic system performs an immune function by transporting immune cells that patrol the tissues to the lymphoid organs (Witte *et al.*, 2001). Insufficiency or obstruction of the lymphatics results in lymphedema, characterized by disabling swelling of the affected tissues. In addition, in many types of cancer, the lymphatic vessels provide a major pathway for tumor metastasis, and regional lymph node metastasis has been shown to be correlated with cancer progression (Karpanen and Alitalo, 2001).

Despite the importance of lymphatic vessels in both normal and pathological conditions, progress in the study of lymphangiogenesis had been hampered by the lack of specific markers. Recent studies have revealed the various transcriptional and signaling components that play important roles in lymphatic development. Embryonic lymphatic endothelial cells (LECs) arise by sprouting from the jugular veins and migrate to form primary lymphatic plexus (Oliver, 2004). In E10 mouse embryos, the *prospero*-related transcription factor Prox1 is expressed in a subset of ECs of the cardinal vein, from which they sprout to form primary lymph sacs (Wigle and Oliver, 1999; Wigle *et al.*, 2002). In *Prox1*-null mice, sprouting of LECs from the veins appears unaffected at embryonic day (E)10.5, but their migration is arrested at around E11.5–E12.0, leading to a complete absence of the lymphatic vasculature. Being a homeobox transcription factor, Prox1 has been shown to up-regulate the expression of lymphatic endothelial cell (LEC) markers, and to down-regulate blood vascular endothelial cell (BEC) markers in mature BECs (Hong *et al.*, 2002; Petrova *et al.*, 2002). These findings suggest that Prox1 regulates the program of differentiation of embryonic BECs to LECs by reprogramming the profiles of expression of specific markers of BECs and LECs. However, it is unclear which target genes elicit the functions of Prox1 during the process of lymphangiogenesis. Lymphangiogenesis is absent in the mice lacking some of Prox1 target genes including podoplanin and vascular endothelial growth factor receptor 3 (VEGFR3).

VEGFR3 serves as a receptor for lymphatic-specific VEGFs, VEGF-C and VEGF-D. VEGF-C is important for normal development of the lymphatic vessels, because deletion of *Vegfc*

This article was published online ahead of print in *MBC in Press* (http://www.molbiolcell.org/cgi/doi/10.1091/mbc.E06-09-0780) on February 7, 2007.

[D] [V] The online version of this article contains supplemental material at *MBC Online* (http://www.molbiolcell.org).

Address correspondence to: Kohei Miyazono (miyazono-ind@umin.ac.jp).

Abbreviations used: EC, endothelial cell; ESC, embryonic stem cell; PECAM1, platelet-endothelial cell adhesion molecule 1; SMA, α-smooth muscle actin; VEGF, vascular endothelial growth factor; BEC, blood vascular endothelial cell; LEC, lymphatic endothelial cell.

leads to complete absence of the lymphatic vasculature in mouse embryos (Karkkainen *et al.*, 2004). In *Vegfc*-null mice, LECs initially differentiate in the cardinal veins but fail to migrate and to form primary lymph sacs, suggesting that VEGF-C is an essential chemotactic and survival factor during embryonic lymphangiogenesis. *Vegfr3* deletion leads to defects in blood-vessel remodeling and embryonic death at midgestation, indicating its importance during early blood vascular development (Dumont *et al.*, 1998).

Recently, integrin $\alpha 9\beta 1$ was shown to function as a receptor for VEGF-C and VEGF-D (Vlahakis *et al.*, 2005). *Integrin* $\alpha 9$-null mice die at 6–12 d of age from bilateral chylothorax, suggesting an underlying defect in lymphatic development (Huang *et al.*, 2000). Furthermore, integrin $\alpha 9$ was shown to be a target gene of the signals mediated by hepatocyte growth factor (HGF), which induces neo-lymphangiogenesis during tissue repair and inflammation (Kajiya *et al.*, 2005). Neo-lymphangiogenesis is also induced by two types of receptor tyrosine kinases, platelet-derived growth factor receptor β (PDGFRβ), which serves as one of receptors for PDGF-BB (Cao *et al.*, 2004) and fibroblast growth factor receptor 3 (FGFR3), which serves as one of receptors for FGF-2 (Shin *et al.*, 2006). Notably, Prox1 has recently been shown to induce FGFR3 expression in BECs (Shin *et al.*, 2006).

Although various signaling cascades have been implicated in embryonic and/or adult lymphangiogenesis, their relationships with Prox1 remain largely unknown. Furthermore, although Prox1 has been shown to activate VEGF-C/VEGFR3 and FGF-2/FGFR3 signals, the direct effects of Prox1 on the behavior of ECs have not yet been elucidated. To address these questions, we expressed Prox1 in two types of ECs, mouse embryonic stem cell (ESC)-derived ECs and human umbilical venous endothelial cells (HUVECs). We found that Prox1 expression regulates the chemotaxis, sheet formation, and migration of ECs by modulating the expression of vascular and lymphatic signaling components and for the first time identified integrin $\alpha 9$ as a target gene of Prox1. Interestingly, our findings revealed that integrin $\alpha 9$ plays a pivotal role in sheet formation by and migration of LECs. These findings were confirmed in developing mouse embryos, suggesting their in vivo significance. Furthermore, knockdown of Prox1 expression in LECs resulted in decrease in the expression of VEGFR3 and integrin $\alpha 9$, leading to the decreased chemotaxes toward VEGF-C. These findings suggest that Prox1 alters the characteristics of BECs and maintains those of LECs by regulating multiple signaling cascades implicated in lymphangiogenesis.

MATERIALS AND METHODS

Cell Culture and Adenovirus Infection

Establishment of Tc-inducible ES cell lines from parental MGZ5TcH2 cells was as described (Masui *et al.*, 2005). Maintenance, differentiation, culture, and cell sorting of MGZ5 ES cells were as described (Yamashita *et al.*, 2000). VEGF-A (30 ng/ml), VEGF-C (300 ng/ml), PDGF-BB (10 ng/ml), and tetracycline (1 μg/ml) were used in each experiment unless otherwise described. HUVECs were obtained from Sanko Junyaku and cultured as described (Ota *et al.*, 2002). Human dermal lymphatic endothelial cells (HDLECs) were obtained from Clonetics (San Diego, CA) and cultured in endothelial basal medium (EBM) containing 5% fetal bovine serum (FBS) and EC growth supplements (Clonetics). Recombinant adenoviruses with wild-type and mutant mouse Prox1 were generated and used as described (Fujii *et al.*, 1999).

RNA Interference and Oligonucleotides

Small interfering RNAs (siRNAs) were introduced into cells as described previously (Koinuma *et al.*, 2003). The target sequence for human Prox1 siRNA was 5′-CACCTTATTCGGGAAGTGCAA-3′. Control siRNAs were obtained from Ambion (Austin, TX).

Immunohistochemistry and Western Blot Analysis

Monoclonal antibodies to platelet-endothelial cell adhesion molecule 1 (PECAM1; Mec13.3) and α-smooth muscle actin (SMA; 1A4) for immunohistochemistry were purchased from BD PharMingen (San Diego, CA) and Sigma (St. Louis, MO), respectively. Staining of cultured cells was performed as described (Yamashita *et al.*, 2000). Stained cells were photographed using a phase-contrast microscope (Model IX70; Olympus, Melville, NY) or a confocal microscope (Model LSM510 META; Carl Zeiss MicroImaging, Thornwood, NY). All images were imported into Adobe Photoshop (San Jose, CA) as JPEGs or TIFFs for contrast manipulation and figure assembly. Antibodies to FLAG and α-tubulin for Western blot analysis and immunohistochemistry were obtained from Sigma. Antibodies to mouse VEGFR3, podoplanin, human VEGFR3, and Prox1 for Western blot analysis and immunohistochemistry were obtained from eBioscience (San Diego, CA), RDI (Flanders, NJ), Santa Cruz Biotechnology (Santa Cruz, CA), and Chemicon (Temecula, CA), respectively. Western blot analysis was performed as described (Kawabata *et al.*, 1998).

Fluorescence-activated Cell Sorting

To sort the LECs and BECs, we performed fluorescence-activated cell sorting (FACS) of mouse embryo cells with an FACS Vantage (Becton Dickinson, Mountain View, CA) as described previously (Morisada *et al.*, 2005). Briefly, E14 mouse embryos were dissociated and subjected to antibody staining for CD45-peridinin chlorophyll protein (PerCP) cyanine 5.5 (Cy5.5) to sort CD45-nonhematopoietic cells for further analysis. Subsequently, the cells were incubated with biotinylated anti-LYVE-1 antibodies (ALY7) followed by allophycocyanin-conjugated streptavidin (PharMingen, San Diego, CA). For double or triple staining, the cells were stained with CD31-phycoerythrin (PE)/FITC, CD34-PE (PharMingen), and TEK4-PE.14.

RNA Isolation and RT-PCR

Total RNA was prepared with ISOGEN reagent (Nippongene, Tokyo, Japan) according to the manufacturer's instructions and reverse-transcribed by random priming and a Superscript first-strand synthesis kit (Invitrogen, Carlsbad, CA). Quantitative RT-PCR analysis was performed using the GeneAmp 5700 Sequence Detection System (Applied Biosystems, Tokyo, Japan). The primer sequences and expected sizes of PCR products are available online as indicated in Supplementary Table 1.

Migration Assay

Chemotaxis was determined using a Cell Culture Insert (8-μm pore size, BD Biosciences, San Jose, CA). A total of 5×10^4 cells were seeded in medium containing 0.5% serum in the upper chamber and migrated toward various growth factors as chemoattractants in the lower chamber for 4 h. When anti-integrin $\alpha 9\beta 1$-neutralizing antibodies (Chemicon) were tested, cells were dissociated by trypsin/EDTA, incubated with neutralizing antibodies (30 μg/ml), and seeded in the upper chamber. Cells in the upper chamber were carefully removed using cotton buds, and cells at the bottom of the membrane were fixed and stained with crystal violet 0.2%/methanol 20%. Quantification was performed by counting the stained cells. Assays were performed in triplicate at least three times.

Video Time-lapse Microscopy

Time-lapse imaging of migrating cells was performed on a Leica DM IRB microscope (Deerfield, IL) equipped with a hardware-controlled motor stage over 24 h in serum-reduced (0.5%) medium at 37°C/5% CO_2. Images were obtained with a Leica DC 350F CCD camera every 15 min and analyzed using Image J software (National Institutes of Health, Bethesda, MD). Migration of each cell was analyzed by measuring the distance traveled by a cell nucleus over the 24-h time period (Michl *et al.*, 2005). Average migration speed was calculated by analyzing at least 10 cells per group.

RESULTS

Prox1 Expression in ESC-derived ECs Induces Morphological Changes and Inhibits Sheet Formation

To examine the effects of Prox1 expression on embryonic ECs, we used an in vitro vascular differentiation system from mouse ESCs (Yamashita *et al.*, 2000). This system allows us to induce both endothelial and mural cells derived from common progenitors expressing VEGF receptor 2 (VEGFR2, Flk1). Because we wanted to induce the expression of Prox1 in differentiated ECs instead of undifferentiated ESCs, we established ESC lines carrying a tetracycline (Tc)-regulatable Prox1 transgene (Tc-Prox1) or no transgene (Tc-Empty; Supplementary Figure 1A; Masui *et al.*, 2005). Removal of Tc from culture of undifferentiated Tc-Prox1 cells, but

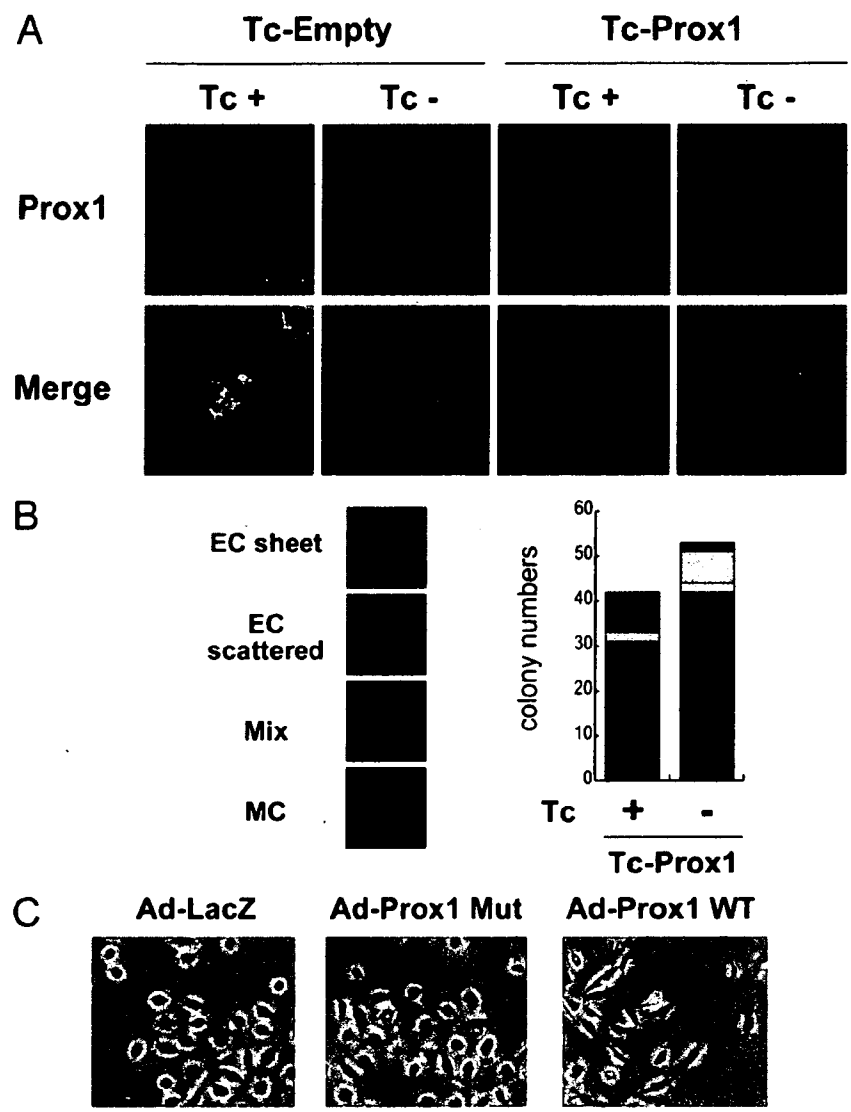

Figure 1. Effect of Tc-regulated Prox1 expression on the morphology and sheet formation of ESC-derived ECs and HUVECs. (A) Flk1+ endothelial progenitor cells were sorted from the differentiated ESCs carrying a Tc-regulated transgene encoding FLAG-epitope-tagged mouse Prox1 (Tc-Prox1) or control transgene (Tc-Empty) and redifferentiated in the presence (+) or absence (−) of Tc to obtain PECAM-1–positive ECs (bottom, red) and smooth muscle α-actin (SMA)-positive mural cells (bottom, green). Expression of FLAG-Prox1 (top, blue) and the morpholoby and sheet formation of ECs (bottom, red) were examined. Scale bars, 100 μm. (B) Quantitation of colony formation, EC and mural cell production, and endothelial sheet formation. Flk1+ cells derived from Tc-Prox1 ESCs were cultured sparsely with 10% fetal calf serum in the absence or presence of Tc for 4 d and stained for PECAM1 (red) and SMA (green). Numbers of different types of colonies per well were counted to determine the effects of Prox1 on colony formation of Flk1+ cells. Four colony types were observed: pure ECs forming sheet structures (EC-sheet, red); pure scattered ECs (EC-scattered, pink); pure mural cells (MC, green); and mixed colonies consisting of endothelial and mural cells (Mix, yellow). Experiments were repeated at least three times with essentially the same results. Bars, 50 μm. (C) Morphology of HUVECs infected with adenoviruses encoding LacZ, DNA-binding mutant (Mut), or wild-type (WT) Prox1. Bars, 100 μm.

not that of Tc-Empty cells, induced the expression of the FLAG epitope-tagged Prox1 gene (Supplementary Figure 1B).

To examine the effects of Prox1 expression on vascular development, we differentiated the Tc-Empty and Tc-Prox1 ES cells into Flk1-expressing (Flk1+) vascular progenitor cells in the presence of Tc, so that no transgene expression is induced. Flk1+ cells were sorted using anti-Flk1 antibodies and were redifferentiated in the presence or absence of Tc. As shown in Figure 1A, Prox1 transgene expression was induced in the vascular cells derived from Tc-Prox1 ES cells only in the absence of Tc. The level of Prox1 transgene expression in ESC-derived vascular cells was approximately twice as high as that of endogenous expression in the LECs derived from E14 mouse embryos (Supplementary Figure S1C). ESC-derived ECs formed a fine cobblestone-like structure of endothelial sheets when Prox1 was not expressed (Figure 1A). However, when Prox1 was expressed, ECs exhibited spindle shapes and failed to form sheet structures.

To further dissect the roles of Prox1 in endothelial sheet formation, we performed quantitative colony formation assays. When Flk1+ cells were plated at a lower density in the presence of VEGF-A, they formed four types of colonies emerging from single Flk1+ cells (Yamashita *et al.*, 2000; Watabe *et al.*, 2003): PECAM1 (CD31)+ pure ECs with or without sheet structure (EC-sheet and EC-scattered, respectively), pure mural cells (MC), and mixtures of both (Mix; Figure 1B). Although the frequencies of pure EC colonies (EC-scattered and -sheet) were ~25% in the absence and presence of Prox1 expression, formation of endothelial sheets was significantly affected by Prox1 (Figure 1B). The frequency of sheet formation among pure endothelial colonies was 82% when single Flk1+ cells were cultured in the absence of Prox1. When Prox1 was expressed, most endothelial colonies exhibited scattered phenotypes (with a frequency of sheet formation of 22%). Furthermore, 95% of sheet-forming ECs derived from Tc-Prox1 ESCs failed to express Prox1 even in the absence of Tc (unpublished data), further suggesting that Prox1 expression in ESC-derived ECs inhibits sheet formation.

Prox1 Induces Morphological Changes and Inhibits Sheet Formation in HUVECs

We next examined whether Prox1 transgene expression also modulates the morphology and sheet formation of HUVECs, which are mature venous ECs. We used adenoviruses encod-

ing wild-type Prox1 (Ad-Prox1WT), a Prox1 mutant containing two amino acid substitutions in its DNA-binding domain (Ad-Prox1Mut) (Petrova *et al.*, 2002), and LacZ (Ad-LacZ) as controls. Levels of expression of wild-type and mutant Prox1 were shown to be comparable at moi 100 (Supplementary Figure 2A) when > 90% of HUVECs were infected (Supplementary Figure 2B). The level of Prox1 transgene expression was shown to be approximately three times as high as that of endogenous Prox1 expression in HDLECs (Supplementary Figure S2, B–D).

The morphology of and sheet formation by HUVECs were also affected by Prox1 (Figure 1C). Although HUVECs infected with adenoviruses encoding LacZ or mutant Prox1 formed a flat cobblestone-like structure, Prox1-expressing HUVECs were spindle-shaped and did not form sheet structures.

Prox1 Expression Increases Motility of ECs

Present findings that Prox1-expressing cells lose a cobblestone-like structure prompted us to examine the effects of Prox1 on the motility of ECs. Tracking single ECs using video time-lapse microscopy showed that Prox1 expression significantly increased the motility of ESC-derived ECs (Supplementary Videos 1 and 2 and Figure 2A) and HUVECs (Supplementary Videos 3 and 4 and Figure 2B). These findings suggest that Prox1 expression results in morphological changes of ECs, inhibition of sheet formation, and induction of EC motility, all of which may be critical phenomena for the progression of embryonic lymphangiogenesis.

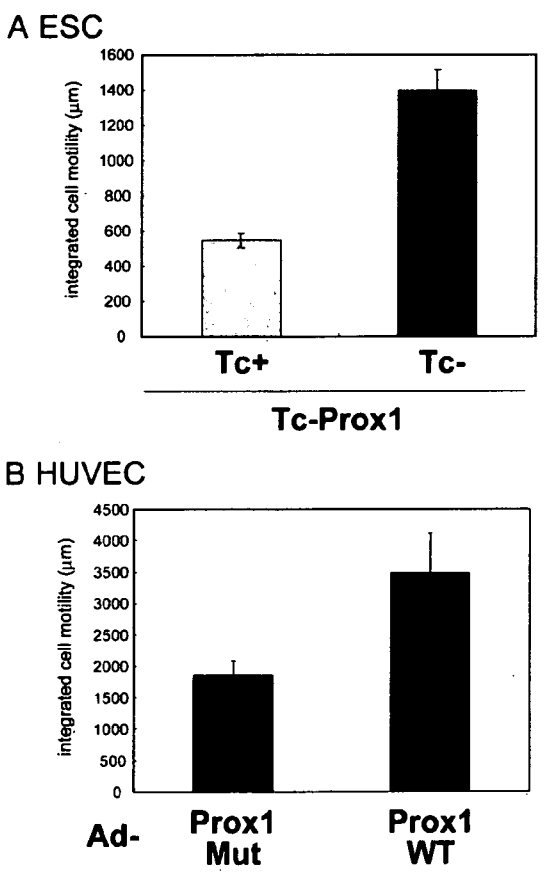

Figure 2. Effects of Prox1 on the migration of ESC-derived ECs and HUVECs. Cell migration was measured by video time-lapse microscopy as described in *Materials and Methods*. (A) ECs derived from Tc-Prox1 ESCs were subjected to video microscopy for 24 h (Supplementary Videos 1 and 2). (B) HUVECs were infected with adenoviruses (Ad) encoding DNA-binding mutant (Mut) or wild-type (WT) Prox1 and subjected to videomicroscopy for 24 h (Supplementary Videos 3 and 4). Results are expressed as the integrated cell motility over 24 h. Each value represents the mean of 10 determinations; bars, SD.

Prox1 Increases Endothelial Motility via Induction of Integrin α9 Expression

We next examined the molecular mechanisms by which Prox1 regulates morphological changes of BECs. Petrova *et al.* (2002) reported that adenovirus-mediated Prox1 expression in human dermal microvascular endothelial cells (HDMECs) resulted in the down-regulation of BEC marker expression and up-regulation of LEC marker expression. We also found that the levels of transcripts for BEC markers (VE-cadherin and VEGFR2) and those for LEC markers (podoplanin and VEGFR3) were down- and up-regulated, respectively, only by Ad-Prox1WT infection in HUVECs, (Supplementary Figure 2), suggesting that Prox1 reprograms the vascular and lymphatic gene expression in HUVECs.

We then examined whether the activation of VEGFR3 signals by Prox1 mediates Prox1-induced morphological changes. However, inhibition of VEGFR3 signals in Prox1-expressing HUVECs by dominant-negative VEGFR3 mutants (Karkkainen *et al.*, 2000) failed to induce reversion of the Prox1-mediated phenotypes (Supplementary Figure 3), suggesting that VEGFR3 signaling is not directly involved in the induction of morphological changes of ECs by Prox1.

Recently, integrin α9, a member of the integrin family that is preferentially expressed in LECs (Petrova *et al.*, 2002), was shown to function as a receptor for VEGF-C and VEGF-D (Vlahakis *et al.*, 2005). Furthermore, *integrin α9*-null mice exhibit defects in lymphatic systems (Huang *et al.*, 2000). Therefore, in order to examine the roles of integrin α9 in the Prox1-mediated morphological changes, we, for the first time, studied the roles of Prox1 in the regulation of integrin α9 expression. As shown in Figure 3, A and B, Prox1 expression increased the expression of integrin α9 in both ESC-derived ECs and HUVECs.

To elucidate the roles played by integrin α9 in the induction of phenotypic changes by Prox1, we used anti-human integrin α9β1 neutralizing (function-blocking) antibodies. Reversion of the morphological changes and decreased sheet formation of HUVECs induced by Prox1 was observed with the addition of anti-integrin α9-neutralizing antibodies to culture (Figure 3C). Furthermore, the increase in motility of HUVECs by Prox1 was lowered to basal level by anti-integrin α9 antibodies (Supplementary Videos 5–8 and Figure 3D). These findings suggest that the phenotypic changes of HUVECs induced by Prox1 are due to increased integrin α9 expression.

Prox1 Increases Chemotaxis to VEGF-C via Induction of Integrin α9 Expression

Because it was recently reported that VEGF-C and VEGF-D are ligands for integrin α9β1 (Vlahakis *et al.*, 2005), we examined whether the up-regulation of integrin α9 expression by Prox1 contributed to the Prox1-induced increase in migration of ECs toward VEGF-C. Chamber migration assays showed that HUVECs expressing wild-type Prox1 migrated toward VEGF-C, and this migration was abrogated by anti-α9β1 neutralizing antibody (Figure 3E), suggesting that Prox1 induces the migration of ECs toward VEGF-C by regulating the expression of integrin α9.

Prox1 Expression Inhibits Chemotaxis of BECs to VEGF-A and Promotes that to VEGF-C via Modulation of their Receptors

Although our findings suggest that signaling from VEGFR3 is not directly involved in Prox1-induced morphological changes

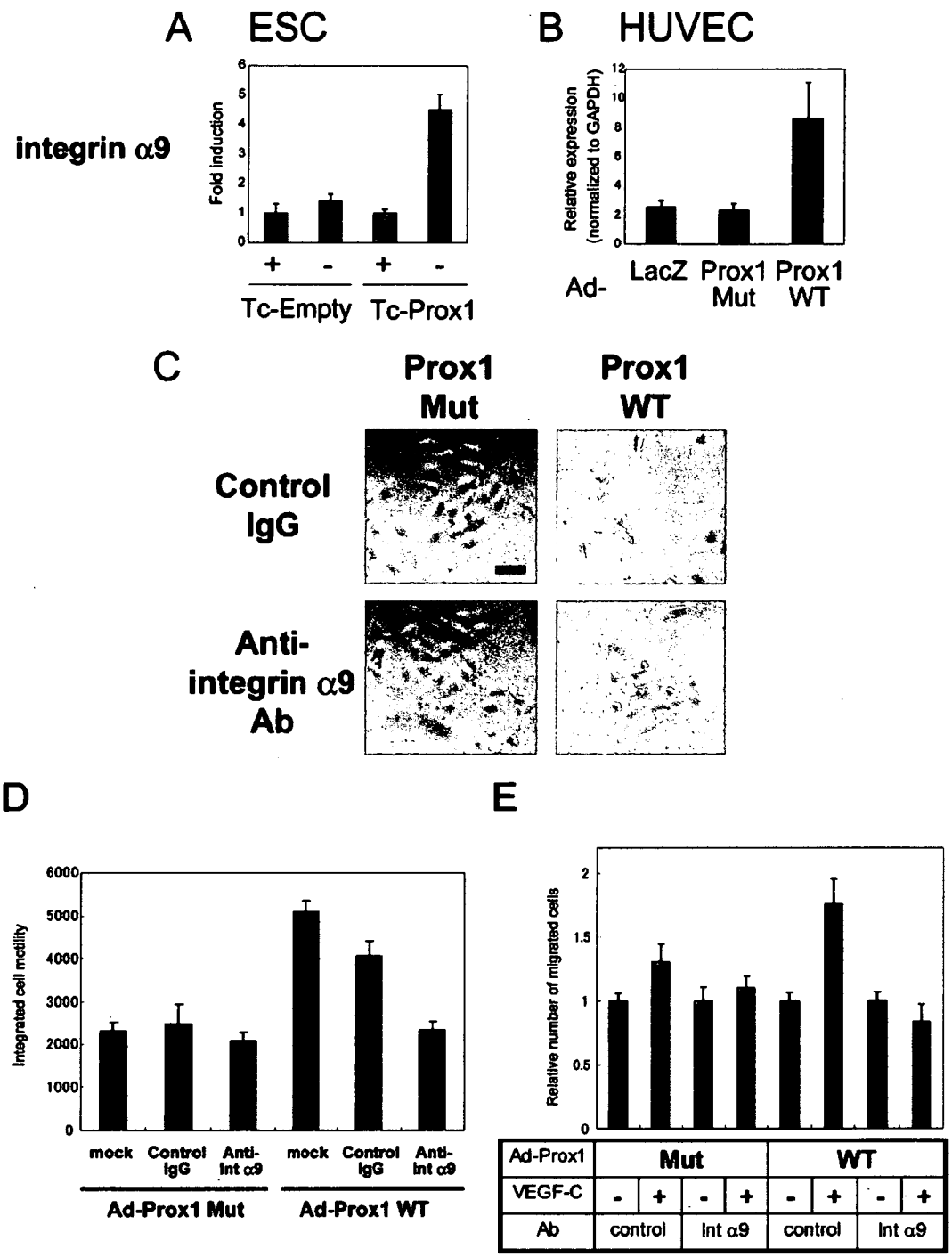

Figure 3. Roles of integrin α9 in the migration of HUVECs. (A and B) Expression of transcripts for integrin α9 was determined by quantitative real-time PCR analysis in ESC-derived ECs (A) and HUVECs (B). (C and D) HUVECs were infected with adenoviruses encoding DNA-binding mutant (Mut) or wild-type (WT) Prox1 and were subjected to videomicroscopy for 24 h in the presence of control IgG or anti-integrin α9 (int α9)-neutralizing antibodies. The final images of HUVECs (C) and integrated cell motility (D) are shown. Bars, 100 μm. Each value represents the mean of 10 determinations; bars, SD (E) Cell migration was measured by Boyden chamber assay. HUVECs were infected with adenoviruses (Ad) encoding DNA-binding mutant (Mut) or wild-type (WT) and plated on Boyden chambers in the presence of control IgG or anti-integrin α9 (int α9)-neutralizing antibodies with VEGF-C placed in lower wells. Results are expressed as the ratio of number of migrated cells normalized to the control (no attractant). Each value represents the mean of triplicate determinations; bars, SD.

(Supplementary Figure 3), it may play important roles in other changes induced by Prox1 in ECs. BECs expressing VEGFR2 and LECs expressing VEGFR3 migrate preferentially toward their ligands VEGF-A and VEGF-C, respectively (Makinen *et*

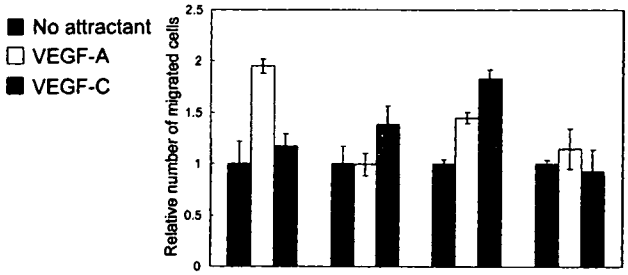

Ad	Prox1	Mut	WT	Mut	WT
	VEGFR3	-	-	WT	d.n. Mut
	Null	+	+	-	-

Figure 4. Effect of Prox1 on the migration of HUVECs stimulated with VEGF-A and VEGF-C. Cell migration was measured by Boyden chamber assay as described in *Materials and Methods*. HUVECs were infected with adenoviruses (Ad) encoding DNA-binding mutant (Mut) or wild-type (WT) Prox1 in combination with those encoding wild-type (WT), dominant-negative mutant form (d.n. Mut) of VEGFR3, or Null (encoding no transcripts) and plated on Boyden chambers with indicated chemoattractants placed in lower wells. Ad-Null was used in order to infect HUVECs with the same quantities of adenoviruses for all of samples. Results are expressed as the ratio of number of migrated cells normalized to control (no attractant). Each value represents the mean of triplicate determinations; bars, SD.

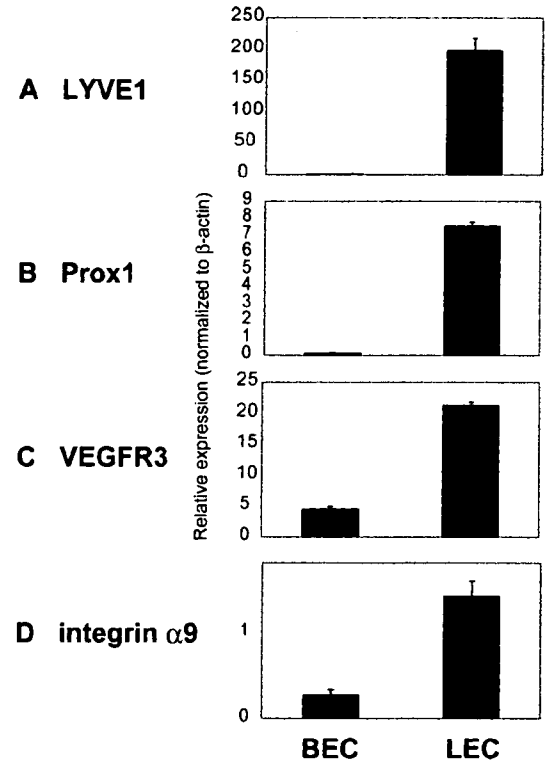

Figure 5. Expression of BEC and LEC markers in Prox1-expressing LECs derived from mouse embryos. E14 mouse embryos were dissected, and embryonic liver and spleen were removed. Other tissues were dissociated and subject to FACS sorting with anti-CD45, LYVE1 (ALY7), CD31, and CD34 antibodies (see *Materials and Methods*). CD45−; CD31+; CD34+; LYVE1− BEC fractions and CD45−; CD31+; CD34−; LYVE1+ LEC fractions were analyzed for the expression of transcripts for LYVE1 (A), Prox1 (B), VEGFR3 (C), and integrin α9 (D) by quantitative real-time PCR analysis. Each value represents the mean of triplicate determinations; bars, SD.

al., 2001). The alteration of expression of VEGFRs in HUVECs by Prox1 prompted us to study their chemoattraction toward VEGFs. Chamber migration assays showed that VEGF-A, but not VEGF-C, stimulated chemotaxis of the HUVECs expressing mutant Prox1 (Figure 4). In contrast, VEGF-C, but not VEGF-A, induced motility of those expressing wild-type Prox1. To examine whether Prox1 induces chemotaxis of HUVECs toward VEGF-C via up-regulation of VEGFR3 expression, we used adenoviruses encoding wild-type and dominant-negative forms of VEGFR3. Expression of wild-type VEGFR3 enhanced chemotaxis of HUVECs toward VEGF-C without altering their migration toward VEGF-A. In addition, inhibition of VEGFR3 signals by the dominant-negative VEGFR3 significantly decreased their chemotaxis toward VEGF-C, which was induced by Prox1. These findings suggest that Prox1 modulates endothelial chemotaxis toward VEGFs via its regulation of VEGFRs expression in addition to that of integrin α9.

Expression of VEGFR3 and Integrin α9 Is Increased in Prox1-expressing LECs from Mouse Embryos

To examine the in vivo significance of our finding that Prox1 induces the expression of VEGFR3 and integrin α9 in ESC-derived ECs, we compared their expression in LECs and BECs derived from E14 mouse embryos. We previously raised monoclonal antibodies against a LEC marker, LYVE-1, and found that sorted CD45-CD31+CD34-lowLYVE-1+ cells derived from E14 mouse embryos represent LECs and that CD45-CD31+CD34+LYVE-1− cells represent BECs (Morisada *et al.*, 2005). We confirmed that expression of LYVE-1 and Prox1 was detected only in sorted LECs (Figure 5). We further examined the expression of Prox1 target genes in LECs and BECs. Expression of VEGFR3 and integrin α9 was detected in the cells in both the LEC and BEC fractions, and their levels of expression in LEC were higher than those in BECs. These findings together suggest that the present in vitro induction by Prox1 of expression of VEGFR3 and integrin α9 may mimic the process of embryonic lymphangiogenesis.

Prox1 Knockdown in LECs Modulates Expression of Lymphatic Endothelial Markers and their Cellular Behavior

Prox1 expression is initiated during embryonic lymphangiogenesis and is maintained in mature LECs, prompting us to examine whether knockdown of Prox1 expression in mature LEC affects their characteristics.

We detected endogenous Prox1 protein in the nuclei of HDLECs, whereas no Prox1 protein was detected in HUVECs (Figure 6A). Expression of transcripts for Prox1, VEGFR3, and integrin α9 was significantly higher in HDLECs than in HUVECs (unpublished data). We next decreased Prox1 levels with siRNAs (Figure 6, B and C). siRNA-mediated decrease of Prox1 led to decrease in the expression of various target genes of Prox1, such as VEGFR3, and integrin α9 (Figure 6, D and E), whereas the expression of most genes including GAPDH was not affected, suggesting that Prox1 maintains the expression of LEC markers in HDLECs.

Mature LECs have been reported to migrate toward VEGF-C (Makinen *et al.*, 2001). To study the effects of Prox1 knockdown on the behavior of HDLECs, we examined their chemotaxis toward VEGFs (Figure 6F). Although HDLECs migrate toward VEGF-A and VEGF-C, Prox1 knockdown caused a specific decrease in the chemotaxis toward VEGF-C (Figure 6F). These results suggest that Prox1 maintains the characteristics of LECs by sustaining the expression of LEC markers.

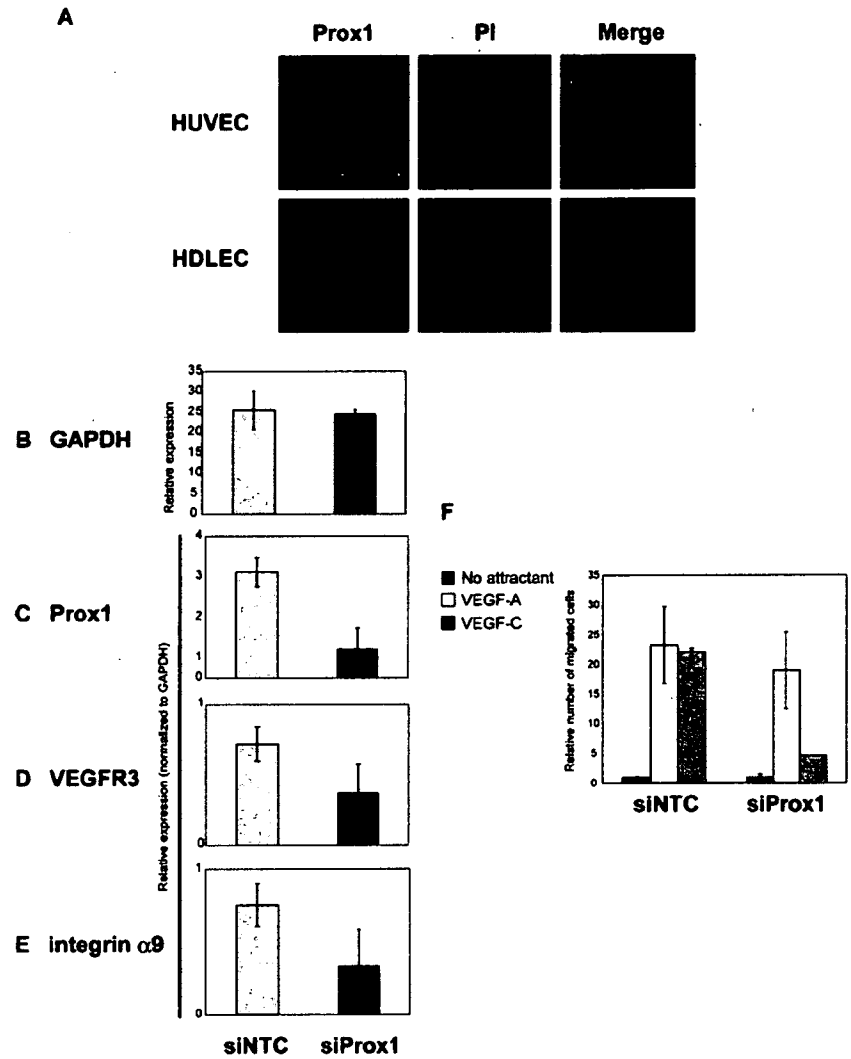

Figure 6. Roles of endogenous Prox1 in HDLECs. (A) Expression of endogenous Prox1 (left; green) was examined by specific antibodies in HUVECs (top) and HDLECs (bottom), with counterstaining for nuclei with propidium iodide (PI, middle; red; and right, merge). Bars, 100 μm. (B–E) Effects of Prox1 knockdown on expression of GAPDH (B), Prox1 (C), VEGFR3 (D), and integrin $\alpha 9$ (E) were examined by quantitative real-time PCR analysis. A scrambled siRNA sequence (Ambion) was used as a negative control siRNA (siNTC). Each value represents the mean of triplicate determinations; bars, SD. (F) Effects of Prox1 knockdown on the chemotaxes of HDLECs toward VEGF-A (50 ng/ml) and VEGF-C (50 ng/ml). Cell migration was measured by Boyden chamber assay as described in *Materials and Methods*. HDLECs were transfected with scrambled siRNAs (siNTC) or Prox1 siRNAs and plated on Boyden chambers with indicated chemoattractants placed in the lower wells. Results are expressed as the ratio of number of migrated cells normalized to control (no attractant). Each value represents the mean of triplicate determinations; bars, SD.

DISCUSSION

Recent studies have revealed that lymphangiogenesis is regulated by various signaling cascades mediated by VEGFs/VEGFRs (Dumont *et al.*, 1998; Karkkainen *et al.*, 2000; Suzuki *et al.*, 2005), and integrin $\alpha 9\beta 1$ (Huang *et al.*, 2000). The present study showed that expression of Prox1 in ECs regulates the expression of various signaling components, including integrin $\alpha 9$, VEGFR2, and VEGFR3, leading to alteration of chemotaxis, sheet formation, and migration of ECs. We also observed that Prox1 modulates the signaling pathways mediated by angiopoietins/Tie2 (Morisada *et al.*, 2005) and FGF/FGFR3 (Shin *et al.*, 2006) in both ESC-derived ECs and HUVECs (unpublished data). In addition, because integrin $\alpha 9$ has been implicated in modulation of signaling cascades mediated by HGF (Kajiya *et al.*, 2005), Prox1 may indirectly modulate HGF signaling. These findings, together with those of previous studies, suggest that Prox1 is a master transcription factor that induces the differentiation of ECs into LECs via regulation of multiple signaling cascades that play important roles in lymphangiogenesis.

Interestingly, we have found that Prox1 induces growth of Flk1+ ECs derived from ESCs, but inhibits the growth of undifferentiated ESCs (unpublished data). These findings suggest that Prox1 requires cell-type–specific modulators for its transcriptional activities and further imply the importance of choosing appropriate endothelial cell types in the identification of Prox1 target genes during embryonic lymphatic differentiation. Although previous studies used mature human dermal ECs to identify target genes of Prox1 (Hong *et al.*, 2002; Petrova *et al.*, 2002), it will be of great interest to use ESC-derived ECs for this purpose.

Alteration of endothelial signaling cascades by Prox1 resulted in decrease in sheet formation, increased motility, and down- and up-regulation of chemotaxis toward VEGF-A and VEGF-C, respectively. An important question is whether these changes mimic the differentiation from BECs to LECs. Blood vascular endothelium and lymphatic endothelium differ in certain specific morphological characteristics. For example, the lymphatic capillaries are larger than the blood capillaries and have an irregular or collapsed lumen, a discontinuous basal lamina, overlapping intercellular junctional complexes, and anchoring filaments that connect the LECs to the extracellular matrix (Witte *et al.*, 2001). The results of morphological observation of in vitro cultured BECs and LECs are controversial. Makinen *et al.* (2001) reported that LECs sorted from human dermal microvascular cells using anti-VEGFR3 antibodies ex-

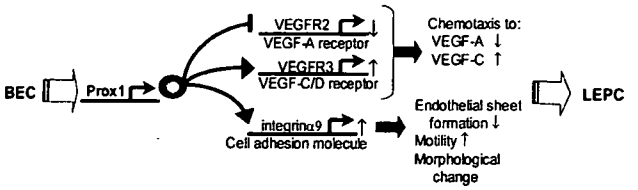

Figure 7. Schematic representation of the roles of Prox1 during the differentiation of blood vessel ECs (BECs) to lymphatic endothelial progenitor cells (LEPCs). See text for details.

hibit elongated cell shapes in the presence of VEGF-C compared with the BECs sorted from the same source. However, Kriehuber *et al.* (2001) reported that LECs sorted from dermal cell suspensions using anti-podoplanin antibodies were not morphologically distinguishable from the BECs sorted from the same source. These differences in findings may be explained by the differences in methods used to isolate and culture LECs and BECs.

During embryonic lymphangiogenesis, Prox1-expressing ECs sprout from cardinal veins and migrate toward VEGF-C–expressing mesenchymal cells (Oliver, 2004). These observations suggest that Prox1-expressing cells need to be mobile to form primary lymphatic sacs. In addition, Prox1 induces proliferation of ESC-derived ECs and HUVECs (unpublished data). However, such cells become stabilized in the VEGF-C–expressing region and form lymphatic capillaries. Furthermore, present work showed that the morphological changes of ECs induced by Prox1 is not dependent on VEGFR3 (Supplementary Figure S3), but on integrin $\alpha 9$ (Figure 3) and that the enhanced chemotaxis toward VEGF-C requires VEGFR3 and integrin $\alpha 9$ (Figures 3 and 4). These findings suggest the hypothesis that Prox1 activates ECs by inducing integrin $\alpha 9$ expression, which results in chemotaxis toward VEGF-C in collaboration with VEGFR3, expression of which is also induced by Prox1, and stabilizes and induces maturation of them via signals mediated mainly by VEGF-C/VEGFR3. This hypothesis is supported by the observation that survival of mature LECs was inhibited by Prox1 knockdown (unpublished data). Prox1 thus appears to function as a master transcription factor for lymphangiogenesis, playing key roles in most of the critical steps during the development of lymphatic sacs, including mobilization, migration, and proliferation of LECs, as well as stabilization of lymphatic capillaries, through modulation of multiple signaling cascades (Figure 7).

The lymphatic vasculature plays important roles in the pathogenesis of various conditions and diseases such as lymphedema and cancer metastasis. The findings of the present study suggest the possibility that expression of Prox1 in BECs and/or endothelial progenitor cells derived from patients may be useful as a therapeutic strategy in regenerative medical treatment of lymphedema. Alternatively, knockdown of Prox1 in cancer patients may inhibit tumor lymphangiogenesis and prevent metastasis.

ACKNOWLEDGMENTS

We thank Drs. J. Yamashita, H. Miki, S. Nishikawa, and members of Department of Molecular Pathology of the University of Tokyo for discussion. This research was supported by Grants-in-Aid for Scientific Research from the Ministry of Education, Science, Sports, and Culture of Japan.

REFERENCES

Cao, R. *et al.* (2004). PDGF-BB induces intratumoral lymphangiogenesis and promotes lymphatic metastasis. Cancer Cell *6*, 333–345.

Dumont, D. J., Jussila, L., Taipale, J., Lymboussaki, A., Mustonen, T., Pajusola, K., Breitman, M., and Alitalo, K. (1998). Cardiovascular failure in mouse embryos deficient in VEGF receptor-3. Science *282*, 946–949.

Fujii, M., Takeda, K., Imamura, T., Aoki, H., Sampath, T. K., Enomoto, S., Kawabata, M., Kato, M., Ichijo, H., and Miyazono, K. (1999). Roles of bone morphogenetic protein type I receptors and Smad proteins in osteoblast and chondroblast differentiation. Mol. Biol. Cell *10*, 3801–3813.

Hong, Y. K., Harvey, N., Noh, Y. H., Schacht, V., Hirakawa, S., Detmar, M., and Oliver, G. (2002). Prox1 is a master control gene in the program specifying lymphatic endothelial cell fate. Dev. Dyn. *225*, 351–357.

Huang, X. Z., Wu, J. F., Ferrando, R., Lee, J. H., Wang, Y. L., Farese, R. V., Jr., and Sheppard, D. (2000). Fatal bilateral chylothorax in mice lacking the integrin alpha9beta1. Mol. Cell. Biol. *20*, 5208–5215.

Kajiya, K., Hirakawa, S., Ma, B., Drinnenberg, I., and Detmar, M. (2005). Hepatocyte growth factor promotes lymphatic vessel formation and function. EMBO J. *24*, 2885–2895.

Karkkainen, M. J., Ferrell, R. E., Lawrence, E. C., Kimak, M. A., Levinson, K. L., McTigue, M. A., Alitalo, K., and Finegold, D. N. (2000). Missense mutations interfere with VEGFR-3 signalling in primary lymphoedema. Nat. Genet. *25*, 153–159.

Karkkainen, M. J. *et al.* (2004). Vascular endothelial growth factor C is required for sprouting of the first lymphatic vessels from embryonic veins. Nat. Immunol. *5*, 74–80.

Karpanen, T., and Alitalo, K. (2001). Lymphatic vessels as targets of tumor therapy? J. Exp. Med. *194*, F37–F42.

Kawabata, M., Inoue, H., Hanyu, A., Imamura, T., and Miyazono, K. (1998). Smad proteins exist as monomers in vivo and undergo homo- and hetero-oligomerization upon activation by serine/threonine kinase receptors. EMBO J. *17*, 4056–4065.

Kriehuber, E., Breiteneder-Geleff, S., Groeger, M., Soleiman, A., Schoppmann, S. F., Stingl, G., Kerjaschki, D., and Maurer, D. (2001). Isolation and characterization of dermal lymphatic and blood endothelial cells reveal stable and functionally specialized cell lineages. J. Exp. Med. *194*, 797–808.

Koinuma, D. *et al.* (2003). Arkadia amplifies TGF-β superfamily signalling through degradation of Smad7. EMBO J. *22*, 6458–6470.

Makinen, T. *et al.* (2001). Isolated lymphatic endothelial cells transduce growth, survival and migratory signals via the VEGF-C/D receptor VEGFR-3. EMBO J. *20*, 4762–4773.

Masui, S., Shimosato, D., Toyooka, Y., Yagi, R., Takahashi, K., and Niwa, H. (2005). An efficient system to establish multiple embryonic stem cell lines carrying an inducible expression unit. Nucleic Acids Res. *33*, e43.

Michl, P. *et al.* (2005). CUTL1 is a target of TGFβ signaling that enhances cancer cell motility and invasiveness. Cancer Cell *7*, 521–532.

Morisada, T. *et al.* (2005). Angiopoietin-1 promotes LYVE-1-positive lymphatic vessel formation. Blood *105*, 4649–4656.

Oliver, G. (2004). Lymphatic vasculature development. Nat. Rev. Immunol. *4*, 35–45.

Ota, T., Fujii, M., Sugizaki, T., Ishii, M., Miyazawa, K., Aburatani, H., and Miyazono, K. (2002). Targets of transcriptional regulation by two distinct type I receptors for transforming growth factor-β in human umbilical vein endothelial cells. J. Cell. Physiol. *193*, 299–318.

Petrova, T. V., Makinen, T., Makela, T. P., Saarela, J., Virtanen, I., Ferrell, R. E., Finegold, D. N., Kerjaschki, D., Yla-Herttuala, S., and Alitalo, K. (2002). Lymphatic endothelial reprogramming of vascular endothelial cells by the Prox-1 homeobox transcription factor. EMBO J. *21*, 4593–4599.

Shin, J. W., Min, M., Larrieu-Lahargue, F., Canron, X., Kunstfeld, R., Nguyen, L., Henderson, J. E., Bikfalvi, A., Detmar, M., and Hong, Y. K. (2006). Prox1 promotes lineage-specific expression of fibroblast growth factor (FGF) receptor-3 in lymphatic endothelium: a role for FGF signaling in lymphangiogenesis. Mol. Biol. Cell *17*, 576–584.

Suzuki, H., Watabe, T., Kato, M., Miyazawa, K., and Miyazono, K. (2005). Roles of vascular endothelial growth factor receptor 3 signaling in differentiation of mouse embryonic stem cell-derived vascular progenitor cells into endothelial cells. Blood *105*, 2372–2379.

Vlahakis, N. E., Young, B. A., Atakilit, A., and Sheppard, D. (2005). The lymphangiogenic vascular endothelial growth factors VEGF-C and -D are ligands for the integrin $\alpha 9\beta 1$. J. Biol. Chem. *280*, 4544–4552.

Watabe, T., Nishihara, A., Mishima, K., Yamashita, J., Shimizu, K., Miyazawa, K., Nishikawa, S., and Miyazono, K. (2003). TGF-β receptor kinase inhibitor enhances growth and integrity of embryonic stem cell-derived endothelial cells. J. Cell Biol. *163*, 1303–1311.

Wigle, J. T., and Oliver, G. (1999). Prox1 function is required for the development of the murine lymphatic system. Cell *98*, 769–778.

Wigle, J. T., Harvey, N., Detmar, M., Lagutina, I., Grosveld, G., Gunn, M. D., Jackson, D. G., and Oliver, G. (2002). An essential role for Prox1 in the induction of the lymphatic endothelial cell phenotype. EMBO J. *21*, 1505–1513.

Witte, M. H., Bernas, M. J., Martin, C. P., and Witte, C. L. (2001). Lymphangiogenesis and lymphangiodysplasia: from molecular to clinical lymphology. Microsc. Res. Tech. *55*, 122–145.

Yamashita, J., Itoh, H., Hirashima, M., Ogawa, M., Nishikawa, S., Yurugi, T., Naito, M., Nakao, K., and Nishikawa, S. (2000). Flk1-positive cells derived from embryonic stem cells serve as vascular progenitors. Nature *408*, 92–96.

The Prostate 68:139–151 (2008)

Deletion of PSCA Increases Metastasis of TRAMP-Induced Prostate Tumors Without Altering Primary Tumor Formation

Miranda L. Moore,[1] Michael A. Teitell,[2] Yoon Kim,[3] Tetsuro Watabe,[3] Robert E. Reiter,[4] Owen N. Witte,[3,5,6]** and Purnima Dubey[1]*

[1]*Department of Pathology, Section on Tumor Biology, Wake Forest University Health Sciences, Winston-Salem, North Carolina*
[2]*Department of Pathology and Laboratory Medicine, University of California, Los Angeles, California*
[3]*Howard Hughes Medical Institute, University of California, Los Angeles, California*
[4]*Department of Urology, University of California, Los Angeles, California*
[5]*Department of Molecular and Medical Pharmacology, University of California, Los Angeles, California*
[6]*Department of Microbiology and Molecular Genetics, University of California, Los Angeles, California*

BACKGROUND. Prostate stem cell antigen (PSCA) is expressed in normal epithelium of various tissues, in embryos and adult animals. PSCA expression is upregulated in up to 70% of prostate tumors and metastases, and a subset of bladder and pancreatic cancers. However, its function is unknown. We studied the effect of targeted gene deletion of PSCA on normal organ development and prostate carcinogenesis.

METHODS. PSCA +/+, PSCA +/−, and PSCA −/− mice were bred and aged to 22 months. A cohort of animals was treated with γ-irradiation at 2 and 6 months of age. PSCA knockout mice were crossed to TRAMP mice and TRAMP+ PSCA +/+, TRAMP+ PSCA +/−, and TRAMP+ PSCA −/− mice and offspring aged to 10 months of age. Tissues were analyzed by RT-PCR, histology, and immunohistochemistry for markers of proliferation, apoptosis, angiogenesis, and tumor progression.

RESULTS. PSCA knockout animals were viable, fertile and indistinguishable from wild-type littermates. Spontaneous or radiation-induced primary epithelial tumor formation was also similar in wild-type and PSCA knockout mice. We observed an increased frequency of metastasis in TRAMP+ PSCA heterozygous and knockout mice, compared to TRAMP+ wild-type mice. Metastases were largely negative for PSCA and androgen receptor. Cleaved-caspase 3 and CD31 staining was similar in all genotypes. Aurora-A and Aurora-B kinases were detected in the cytoplasm of PSCA heterozygous and knockout tumors, suggesting aberrant kinase function.

This article contains supplementary material, which may be viewed at the The Prostate website at http://www.interscience.wiley.com/jpages/0270-4137/suppmat/index.html.

Grant sponsor: WFUHS; Grant sponsor: CaP CURE (now Prostate Cancer Foundation); Grant sponsor: Prostate Cancer Foundation; Grant sponsor: NCI Mouse Models for Human Cancers Consortium; Grant number: P50 CA92131; Grant sponsor: NIH/NCI; Grant number: U01 CA084128; Grant sponsor: NIH; Grant numbers: R01CA90571, R01CA107300.

Yoon Kim's present address is University of California, Irvine, CA.

Tetsuro Watabe's present address is Department of Molecular Pathology, Graduate School of Medicine, University of Tokyo, 7-3-1 Hongo, Bunkyo-ku, Tokyo 113-0033, Japan.

*Correspondence to: Purnima Dubey, PhD, Department of Pathology, Section on Tumor Biology, Wake Forest University Health Sciences, Medical Center Blvd., 2100 Gray Building, Winston-Salem, NC. E-mail: pdubey@wfubmc.edu

**Correspondence to: Owen N. Witte, MD, Department of Microbiology and Molecular Genetics, Howard Hughes Medical Institute, University of California, Los Angeles, CA; 675 Charles E. Young Dr. South, 5-720 MRL, Los Angeles, CA 90095-1662.
E-mail: owenw@microbio.ucla.edu

Received 5 June 2007; Accepted 11 September 2007
DOI 10.1002/pros.20686
Published online 28 November 2007 in Wiley InterScience (www.interscience.wiley.com).

CONCLUSION. These data suggest that PSCA may play a role in limiting tumor progression in certain contexts, and deletion of PSCA may promote tumor migration and metastasis. *Prostate 68: 139–151, 2008.* © 2007 Wiley-Liss, Inc.

KEY WORDS: **PSCA; metastasis; gene deletion; GPI-anchored protein; prostate cancer**

INTRODUCTION

Prostate cancer is the second leading cause of cancer-related death in American men [1]. Current therapy includes radical prostatectomy and androgen ablation therapy, which treat the primary tumor [2,3], but are ineffective against androgen-independent disease that can arise later.

Several cell-surface proteins identified on primary prostate tumors and metastases [4,5], serve as targets for antibody-mediated therapy. One target is prostate stem cell antigen (PSCA; [6]), a cell surface GPI-anchored protein with homology to stem cell antigen 2 (Sca-2), expressed on immature lymphocytes [7]. Extensive analysis by several groups showed that PSCA is expressed in epithelial cells of a restricted set of organs, and revealed similar patterns of expression for human PSCA (hPSCA) and its murine homologue (mPSCA). In adult tissues, hPSCA and mPSCA are expressed in epithelial cells of bladder, stomach and prostate [8]. Beginning at embryonic day 14, mPSCA message is found in the GI tract and urogenital sinus (UGS) [8]. mPSCA expression in prostate is highest in the prostates of young (5- to 8-week-old) mice, and undetectable by 16 weeks of age [8,9]. Furthermore, environmental signals such as castration modulate PSCA expression [9,10].

mPSCA levels increase dramatically in cancers that develop in the TRAMP and PTEN mouse models of prostate cancer [8,9,11]. By in situ hybridization and flow cytometry, up to 70% of cancer epithelial cells express PSCA, while it is barely detectable in age-matched normal prostate tissue.

Similarly, varying levels of hPSCA message and protein [12,13] are detected in more than 50% of primary prostate cancer and metastases, 50% of bladder cancers [14,15], and 60% of pancreatic cancers [16]. It was suggested recently that PSCA overexpression is a correlate of more aggressive disease and a poor prognosis [17].

In vitro, antibody binding to the extracellular portion of PSCA can transmit a cytotoxic signal [18]. In xenograft models, antibodies against hPSCA can prevent tumor growth [19] and cause regression of established tumors [20], suggesting that anti-PSCA antibodies may have clinical utility [21].

Despite extensive expression analysis, the biological function of PSCA is unknown. PSCA is a member of the Ly6 family of GPI-anchored proteins, which comprises at least nine other members [22], with roles in hematopoietic stem cell development and lymphocyte activation. Sca-1 knockout mice show defective hematopoietic stem cell and progenitor defects [23]. High expression of Sca-2 and low expression of four other family members is detected in normal prostate [24], suggesting a role for Ly6 family members in prostate development. Given these data, we investigated whether genetic deletion of PSCA would affect normal urogenital development. We observed that PSCA knockout mice are viable, and fertile with normal litters, suggesting that PSCA is not critical for development or normal urogenital function.

The Ly6 proteins and homologs may play a role in cancer progression. High Ly6E expression is correlated with a highly malignant tumor phenotype, while low Ly6E levels are correlated with low malignant potential of fibroblast tumor and mammary adenocarcinoma cells [25]. Overexpression of urokinase plasminogen activator receptor (uPAR) is associated with cell invasion and migration [26]. C4.4A has low homology to uPAR, and binding of C4.4A by its ligands laminin 1 and laminin 5, results in cell spreading and migration [27].

Continued maintenance of a protein throughout the disease suggests a functional role in disease development or progression. To evaluate the effect of PSCA deletion on spontaneous tumor development, we aged PSCA wild-type, heterozygous and knockout mice to 2 years of age. Surprisingly, the tumor incidence and spectrum was similar in aged mice of all three genotypes. Treatment with sublethal gamma irradiation to provide a second "hit" also did not change the frequency or tumor spectrum in old PSCA heterozygous or knockout mice, compared to wild-type mice. Thus, PSCA does not inhibit or accelerate primary tumor formation.

To further assess the effect of PSCA deletion when tumor development was initiated by a defined oncogene, we crossed PSCA −/− mice to *T*ransgenic *A*denocarcinoma of the *M*ouse *P*rostate (TRAMP [28]) mice. We collected and aged mice to 40 weeks of age. TRAMP+ PSCA +/+, PSCA +/−, and PSCA −/− mice all developed primary prostate cancer. On autopsy and histological examination we detected metastases to liver, kidney and lung in 61.3% of PSCA +/− and 56.25% of PSCA −/− TRAMP transgenic

mice and only 33% of TRAMP+ PSCA +/+ mice. Quantitative RT-PCR analysis showed lower levels of mPSCA in metastases of PSCA +/− mice than in primary tumors or normal prostate. Immunohistochemical analysis for CD31 and cleaved caspase-3 showed similar levels of angiogenesis and apoptosis, respectively, for all three genotypes. IHC for Aurora-A, Aurora-B, and Survivin as markers of tumor progression revealed largely cytoplasmic localization of all three proteins in TRAMP+ PSCA +/− and TRAMP+ PSCA −/− tumors. Together, these data show that genetic deletion of PSCA correlates with metastatic spread from the primary tumor.

MATERIALS AND METHODS

Mice

Animals were maintained in accordance with the Institutional Animal Care and Use Committee of UCLA and WFUHS. PSCA knockout mice (129/Sv strain background, Transgenic Mouse Facility, University of California, Irvine) were maintained on a mixed 129/Sv × C57BL/6 background. C57BL/6 background TRAMP transgenic mice (Jackson Labs, Bar Harbor, Maine) were genotyped by PCR of tail genomic DNA.

To generate PSCA +/+, +/− and −/− mice, male and female PSCA knockout mice were crossed to C57BL/6 mice. F1 PSCA +/− mice were intercrossed, to generate the F2 generation of PSCA +/+, +/− −/− mice, and screened by Southern blot analysis of tail genomic DNA.

PSCA knockout mice were crossed to TRAMP transgenic mice carrying one copy of the transgene. TRAMP+ PSCA +/− (F1) mice were crossed to TRAMP− PSCA +/− mice to ensure that the F2 generation carried one copy of the transgene and that background genes distributed randomly.

Autopsy and Tissue Harvest

Animals were killed when they displayed distended abdomens, weight loss, slow gait, ruffled fur, or labored breathing. All tissues, femur and spine were harvested. Portions of each tissue were fixed in formalin for histology, snap-frozen in liquid nitrogen for RNA extraction, and incubated in DNA extraction buffer (0.5M EDTA, 2M Tris pH 8.0, 10% SDS, 600 μg/ml Proteinase K) for genomic DNA isolation.

Histopathology and Immunohistochemistry

Sections (5 μm) were stained with hematoxylin and eosin, and evaluated by MAT in a blinded analysis using published criteria [29,30]. Statistical significance was determined by two-tailed Student's *t*-test.

IHC analysis of 5 μm tissue sections for expression of T antigen, androgen receptor (AR), Ki67, CD31, cleaved caspase-3, Aurora-A, Aurora-B, and Survivin was performed with minor modifications of manufacturers' and published protocols [29,31]. Antigen was unmasked by boiling (98°C water bath for 30 min) or incubation in a pressure cooker in citrate buffer. Antibody sources: T antigen, CD31, BD Pharmingen (San Diego, CA); AR, Upstate Biotechnology (Lake Placid, NY), Ki67, Lab Vision Corporation (Fremont, CA); Aurora-A, Bethyl Laboratories (Montgomery, TX); Aurora-B, Novus Biologicals (Littleton, CO); survivin (gift of Dr. Hugo Caldas, WFUHS), Santa Cruz Biotechnology (Santa Cruz, CA); cleaved caspase-3, Cell Signaling Technologies (Danvers, MA).

Quantification of Immunohistochemical Staining

Stained sections were quantified using ImageJ software (http://rsb.info.nih.gov/ij/). Stained sections were photographed at 400× magnification. Representative fields were chosen randomly, a grid applied, and 150 cells with nuclei were quantified. For AR, Ki67, CD31 and cleaved-caspase 3, the number of positive cells/150 in a field were determined. For Aurora-A, Aurora-B, and Survivin, the distribution of nuclear versus cytoplasmic staining was determined. An average and standard deviation were calculated, and statistical significance was determined using a two-tailed *t*-test with $P < 0.05$ considered significant.

Preparation of RNA and DNA

Total RNA was extracted from snap-frozen tissues using the RNeasy kit (Qiagen, Valencia, CA) following manufacturer's protocol. Genomic DNA was isolated using the Wizard Genomic DNA Purification Kit (Promega, Madison, WI). RNA and DNA were quantified by $OD_{260/280}$.

RT-PCR

First-strand cDNA was synthesized using an oligo d(T) primer and Superscript II Reverse Transcriptase (Invitrogen, Carlsbad, CA). Semi-quantitative PCR for mPSCA was performed using standard conditions, with primers specific for the mature portion of mPSCA.

mPSCA-GST-5′: 5′-GGAGAATTCATGCTCTGCAGTGCTATTCATGC-3′; mPSCA-GST-3′: 5′-GGAGAATTCCTAGGTGTGGGCCCCGTTGAC-3′. Product was normalized to murine beta actin. Actin primers, b-actin-FWD: 5′-CACAGGCATTGTGATGCACT, b-actin-REV: 5′-CTTCTGCATCCTGTCAGCCAA-3′. Quantitative PCR was performed using a Model 7700 instrument (Applied Biosystems, Foster City, CA), and TaqMan Gene Expression Assays

(Applied Biosystems) for mPSCA and murine β-actin. Amplicons were detected using FAM dye-labeled probes. Twenty microliters reaction volumes included 2X Taqman Universal PCR Master Mix (Applied Biosystems) 20X Assay Mix and varying concentrations of first-strand cDNA. Individual RNA samples were normalized to the levels of β-actin message.

RESULTS

Deletion of PSCA Does Not Affect Viability or Fertility in PSCA Knockout Mice

The PSCA knockout targeting construct was generated by substituting all of exon 2 and a portion of exon 3 with the neomycin gene (Fig. 1A). Embryonic expression of PSCA in the UGS and GI tract [8,10] suggested a role for PSCA in epithelial cell differentiation. Surprisingly, however, PSCA knockout mice were viable and developed to adulthood. RT-PCR analysis of prostate and bladder confirmed absence of PSCA in knockout mice (data not shown).

H&E-stained sections of 7- and 10-week-old prostate lobes of PSCA +/− and PSCA −/− mice were similar in size and structure to wild-type mice (Fig. 1B). Wet weights of the male UGS were similar in all three PSCA genotypes (data not shown). PSCA expression is modulated by changes in systemic androgen [32]. Prostate involution after castration and regeneration after addition of exogenous androgen was normal in PSCA knockout mice (data not shown). Male and female knockout mice are fertile, with normal litter size and gender distribution (data not shown), showing that PSCA deletion does not interfere with normal urogenital function.

Incidence and Distribution of Malignancy Is Similar in Aged PSCA +/+, +/−, and −/− Mice

We examined whether deletion of PSCA altered the frequency, latency, or spectrum of tumors in mice aged to 22 months of age. We collected groups of 10–15 PSCA +/+, +/−, and −/− male mice from the F2 generation. Table I shows the age at analysis and associated pathology for each group of animals. No tumors were detected in 30–40% of the animals of any of the genotypes. PIN was observed in wild-type, heterozygous and knockout mice at a similar frequency, and adenocarcinoma in only one animal of each group. One wild-type and one heterozygous animal developed a lung adenocarcinoma. Together, the incidence and distribution of tumors in PSCA heterozygous and knockout mice was very similar to wild-type littermates. Therefore, our results show that deletion of PSCA alone is insufficient to initiate or inhibit cancer development.

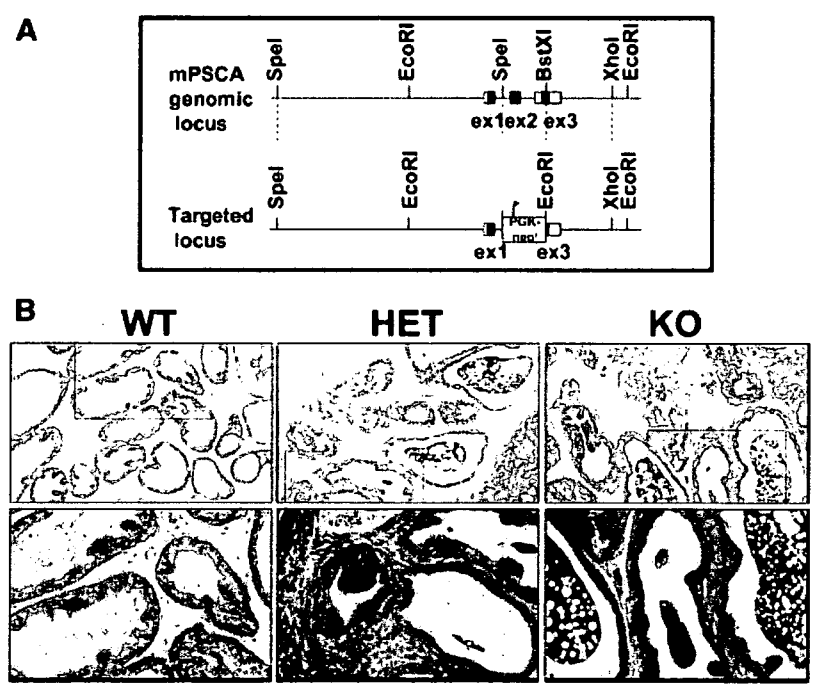

Fig. 1. Prostate development in PSCA heterozygous and knockout mice is normal. **A**: The PSCA knockout allele was created by replacing most of exon 2 and all of exon 3 by the neomycin gene. **B**: Histological examination of prostates from PSCA wild-type (WT), heterozygous (HET), and knockout (KO) mice shows normal glandular architecture. **Upper panels**, 100× magnification. **Lower panels**, 200× magnification. Box in upper panel indicates area of magnification.